American Society of Hematology
2021 L Street NW, Suite 900,
Washington, DC 20036
Phone: 202-776-0544 | Fax 202-776-0545
editorial@hematology.org

Non-canonical EZH2 drives retinoic acid resistance of variant acute promyelocytic leukemias

Tracking no: BLD-2022-015668R2

Mathilde Poplineau (AIX MARSEILLE UNIVERSITY, France) Nadine Platet (Inserm, France) Adrien Mazuel (AIX MARSEILLE UNIVERSITY, CRCM, France) Léonard Hérault (AIX MARSEILLE UNIVERSITY, CRCM, France) Lia N'GUYEN (CRCM, France) Shuhei Koide (Chiba University, Japan) Yaeko Nakajima-Takagi (Chiba University,) Wakako Kuribayashi (National Institute on Aging, United States) Nadine CARBUCCIA (INSERM, France) Loreen Haboub (Inserm, France) Julien VERNEREY (CRCM, France) Motohiko Oshima (Chiba University, Japan) Daniel Birnbaum (CRCM, IPC, France) Atsushi Iwama (Chiba University, Japan) Estelle Duprez (CRCM, IPC, France)

Abstract:
Cancer cell heterogeneity is a major driver of therapy resistance. To characterize resistant cells and their vulnerabilities, we studied the PLZF-RARA variant of acute promyelocytic leukemia (APL), resistant to retinoic acid (RA), using single-cell multi-omics. We uncovered transcriptional and chromatin heterogeneity in leukemia cells. We identified a subset of cells resistant to RA with proliferation, DNA replication and repair signatures, that depend on a fine-tuned E2F transcriptional network targeting the epigenetic regulator Enhancer of Zeste Homolog 2 (EZH2). Epigenomic and functional analyses validated the driver role of EZH2 in RA resistance. Targeting pan-EZH2 activities (canonical/non-canonical) was necessary to eliminate leukemia relapse initiating cells, which underlies a dependency of resistant cells on an EZH2 non-canonical activity and the necessity to degrade EZH2 to overcome resistance. Our study provides critical insights into the mechanisms of RA resistance that allow us to eliminate treatment-resistant leukemia cells by targeting EZH2, thus highlighting a potential targeted therapy approach. Beyond RA resistance and APL context, our study also demonstrates the power of single-cell multi-omics to identify, characterize and clear therapy-resistant cells.

Conflict of interest: No COI declared

COI notes:

Preprint server: Yes; BioRvix https://doi.org/10.1101/2022.01.04.474890

Author contributions and disclosures: M.P. and E.D. developed the original hypothesis and designed experiments. M.P. with the help from N.P., K.S., W.K., L.N., M.O. and N.C. performed experiments and/or analyzed data. A.M and L.H. carried out computational analyses of the scRNA-seq and scATAC-seq. L.H. developed the pipeline for scRNA-seq and scATAC-seq data integration. M.P. and J.V. conducted ChIP-seq analyses. A.I. and D.B. provided reagents and discussed results. M.P., E.D. and A.M. designed the figures and M.P. and E.D. wrote the manuscript. All co-authors proofread the manuscript.

Non-author contributions and disclosures: No;

Agreement to Share Publication-Related Data and Data Sharing Statement: The raw ChIP-seq, scATAC-seq and scRNA-seq data (fastq files) are deposited under the accession number GSE181190. Token for the reviewer ojobcoocxhcjnid The repository also contains the bigwig, the peak matrix and the count matrix for the ChIP-seq, scATAC-seq and scRNA-seq respectively

Clinical trial registration information (if any):

Non-canonical EZH2 drives retinoic acid resistance of variant acute promyelocytic leukemias

Poplineau M.[1,2,6*], Platet N.[1,6], Mazuel A.[1,6†], Hérault L.[1,3,6†], N'Guyen L.[1,6] , Koide S.[2,4], Nakajima-Takagi Y.[2,4] , Kuribayashi W.[2,4] , Carbuccia N.[5], Haboub L.[1,6], Vernerey J.[1], Oshima M.[2,4], Birnbaum D.[5], Iwama A.[2,4] and Duprez E.[1,6*]

[1] Epigenetic Control of Normal and Malignant Hematopoiesis, CRCM, Aix Marseille University, CNRS UMR7258, INSERM U1068, Institut Paoli-Calmettes, Marseille, France

[2] Department of Cellular and Molecular Medicine, Graduate School of Medicine, Chiba University, Chiba 260-8670, Japan

[3] MABioS, I2M, Aix Marseille University, CNRS UMR7373

[4] Division of Stem Cell and Molecular Medicine, Center for Stem Cell Biology and Regenerative Medicine, Institute of Medical Science, University of Tokyo, Tokyo, Japan.

[5] Predictive Oncology Laboratory, CRCM, Aix Marseille University, CNRS UMR7258, INSERM 1068, Institut Paoli-Calmettes, Marseille, France

[6] Equipe Labellisée Ligue Nationale Contre le Cancer

[†]authors equally contributed

*corresponding authors: mathilde.poplineau@inserm.fr; estelle.duprez@inserm.fr

KEYWORDS

Single-cell multi-omics; Leukemia resistance; Retinoic acid; PLZF-RARA; Canonical/non-canonical EZH2

Running Title: Non-canonical EZH2 in leukemia

- **Single cell multi-omics in PLZF-RARA leukemic cells resolves retinoic acid resistance network**
- **Targeting pan-EZH2 activities (canonical/non-canonical) eradicates leukemia relapse-initiating cells**

ABSTRACT

Cancer cell heterogeneity is a major driver of therapy resistance. To characterize resistant cells and their vulnerabilities, we studied the PLZF-RARA variant of acute promyelocytic leukemia (APL), resistant to retinoic acid (RA), using single-cell multi-omics. We uncovered transcriptional and chromatin heterogeneity in leukemia cells. We identified a subset of cells resistant to RA with proliferation, DNA replication and repair signatures, that depend on a fine-tuned E2F transcriptional network targeting the epigenetic regulator Enhancer of Zeste Homolog 2 (EZH2). Epigenomic and functional analyses validated the driver role of EZH2 in RA resistance. Targeting pan-EZH2 activities (canonical/non-canonical) was necessary to eliminate leukemia relapse initiating cells, which underlies a dependency of resistant cells on an EZH2 non-canonical activity and the necessity to degrade EZH2 to overcome resistance.

Our study provides critical insights into the mechanisms of RA resistance that allow us to eliminate treatment-resistant leukemia cells by targeting EZH2, thus highlighting a potential targeted therapy approach. Beyond RA resistance and APL context, our study also demonstrates the power of single-cell multi-omics to identify, characterize and clear therapy-resistant cells.

INTRODUCTION

Acute promyelocytic leukemia (APL) is a class of acute myeloid leukemia (AML) that accounts for 10–15% of all cases and is characterized by recurrent chromosomal translocations involving invariably the gene encoding the Retinoic Acid Receptor alpha (RARA) (17q21) with several fusion partners, such as *PML* (15q22) or *PLZF* (11q23) (For review [1]). The resulting X-RARA fusion proteins were among the first transcription factors (TFs) to be identified as drivers of cancer [2]. They behave as RARA signaling repressors due to their ability to oligomerize and to recruit epigenetic repressors at cis-regulatory DNA regions of RARA target genes and initiate oncogenic gene expression signatures [3]. APL patients with PML-RARA fusion, are exquisitely sensitive to Retinoic Acid (RA) treatment, a sensitivity that has made APL one of the most successful examples of targeted therapy to mutational events [4; 5]. However, APL variant cases, such as the t(11;17), which represent 1% of APL cases still poses clinical challenges [6], as they respond poorly to RA and remain clinically resistant [7].

Contrary to PML-RARA APL, pharmacological doses of RA, although inducing partial differentiation of the PLZF-RARA blasts, do not clear the Leukemia Initiating cell (LIC) of this APL variant [8, 9]. This highlighted the uncoupling between blast differentiation and tumor eradication. The PLZF moiety of the fusion is thought to play a determinant role in RA-resistance. PLZF is a potent transcriptional repressor that can interact by itself with epigenetic complexes [3; 10]. Given that PLZF binding sites with corepressors are conserved in the PLZF-RARA fusion, one hypothesis is that inappropriate recruitment of functional epigenetic repressors, such as the Polycomb Repressor Complex 1 (PRC1), would trigger epigenetic imbalance at very specific genomic loci in an RA insensitive manner [11]. This is consistent with the observed degradation of PLZF-RARA under RA treatment[12] suggesting a persistent mechanism even in the absence of detectable fusion involving chromatin modifications. However, the molecular basis for the resistance of PLZF-RARA expressing cells and why some cells retain their self-renewal capacity while others do not after RA treatment remain unknown.

To identify actionable vulnerabilities that will prevent resistance and facilitate treatment response, we studied PLZF-RARA APL cellular heterogeneity by integrating scRNA-seq and scATAC-seq data obtained from an RA-treated PLZF-RARA mouse model. Establishing cellular clusters and arranging them in hierarchies helped us to identify a subpopulation of transformed promyelocytes that were insensitive to RA-induced differentiation and characterized by a high expression of Enhancer of Zeste Homolog 2 (EZH2), the catalytic subunit of Polycomb Repressive Complex 2 (PRC2). Because EZH2 is an interesting cancer target [13], we further explored EZH2 function in APL development and RA treatment response. We discovered a dual role of EZH2 in APL onset and RA response, suggesting the need to target the non-histone methyltransferase activity of EZH2 for leukemia clearance.

METHODS

A complete description of all methods is presented in the supplemental Methods.

Mouse models and purification of leukemic cells

The APL mouse model (named here PLZF-RARA model) was previously described by Pandolfi [14]. For transplantation, Cd45.2 APL cells were transplanted in sub-lethally irradiated (1.5 Gy) NSG mice. All-Trans Retinoic Acid (RA) and GSK126 (MedChemExpress) were intraperitoneally administered; RA: 0.8-1 mg per mice for 3 or 7 consecutive days; GSK126: 1.25 mg per mice for 10 consecutive days. Leukemic myeloid progenitors (Promyelocytes: Cd45.2$^+$, C-Kit$^+$, Gr1$^+$; ProReP: Cd45.2$^+$, C-Kit$^+$, Gr1$^+$, Cd48$^+$, Cd11b$^-$; NeuRA : Cd45.2$^+$, C-Kit$^+$, Gr1$^+$, Cd48$^-$, Cd11b$^+$) were purified using the FACS Aria III cell sorter (Beckman Dickinson). APL models were bred and

maintained in the CRCM mouse facility (Marseille, France) in accordance with institutional guidelines and approved by the French authority (authorization number: 23893).

Single-cell analyses were performed on the 10X Genomics platform.

For single-cell RNA-sequencing (scRNA-seq), Promyelocytes were processed with the ChromiumTM Next GEM single cell 3' GEM, Library & Gel bead Kit v2Controller according to the manufacturer's instructions, at a target capture rate of 6,000 individual cells per sample.

For single-cell ATAC-sequencing (scATAC-seq), promyelocyte nuclei were purified according 10X Genomics instructions and processed using the Chromium Next GEM Single Cell ATAC Reagent Kits v1.1 following the manufacturer's protocols at a target capture rate of 10,000 nuclei per sample.

scRNA-seq and scATAC-seq were sequenced using a 75-nt single-end and a 150 nt paired-end protocol, respectively. Data were processed using the 10X software Cell Ranger (v4.0) and the 10X software Cell Ranger ATAC (v1.2.0). The mm10 genome was used as reference.

RESULTS

Single-cell transcriptomic analysis identifies a subset of retinoic acid resistant leukemic cells.

To decipher mechanisms linked to APL t(11;17) RA resistance and identify features of RA-resistant leukemic cells, we performed single-cell RNA sequencing (scRNA-seq) on promyelocytes ($cKit^+$; $Gr1^+$) obtained from bone marrow (BM) of PLZF-RARA-TG transplanted mice, treated or not with RA for 7 days. The impact of RA-treatment was measured by the expression of cell surface markers and the morphology of FACS-sorted promyelocytes (**Figures S1A-S1C**). We identified six clusters that were annotated by enrichment analysis (**Figures 1A-B, S1D**). Five of the clusters had neutrophil associated signatures (Prom1, Prom2, Prom3, NeuRA1, NeuRA2) consistent with the promyelocytic stage of induced leukemia, while one cluster was characterized by genes involved in DNA replication associated with DNA repair and proliferation processes (ReP) (**Figure 1B**, **S1E, Tables S1A-C**). Prom1, Prom2 and Prom3 were enriched with untreated cells suggesting their fading upon RA treatment (**Figure 1C**), while NeuRA1 and NeuRA2 appeared almost exclusively in RA-treated cells. The terminal myeloid differentiation status of these two groups was supported by their gene signature (**Figure S1F**). By contrast the ReP cluster was characterized by the expression of genes involved in homologous recombination and DNA replication such as *Rad51, Pcna* and *Mcm3* (**Figure S1G**) and was equally composed of

NT and RA-treated cells (**Figure 1C**) suggesting that RA treatment did not impact on the cell identity of these promyelocytes.

To determine the potential differentiation journey of the RA-treated transformed promyelocytes, we computationally reconstructed the differentiation trajectory of NT and RA-treated cells (**Figures 1D-F**). We revealed three trajectories split into five different states of promyelocytes (segments A, B, C, D, E) and defined the departure of the trajectories at the extremity of state A, which was mostly composed of ReP cells (**Figure 1D**). Trajectories 1 (states A-C-D) and 2 (states A-C-E) ended towards RA differentiated cells, since their final states C, D and E were largely composed of RA-treated cells grouped in NeuRA1 and NeuRA2, respectively (**Figures 1E-F**). This data confirmed a pronounced differentiating effect of RA on a portion of leukemic cells consistently with a stronger expression of differentiation marker in NeuRA2 (**Figure S1F**). Interestingly, the third trajectory (state B), which went far into the pseudotime was composed mostly of NT cells grouped in Prom2 and Prom3 (**Figures 1E-F**), suggesting a spontaneous differentiation program in leukemic cells. This analysis showed a pronounced but partial differentiating effect of RA on PLZF-RARA expressing cells and designated cells in the ReP cluster as the treatment-persistent cells.

To further investigate the RA (un)responsiveness of the identified clusters, we took advantage of available transcriptional signatures reflecting RA sensitivity of PML-RARA *versus* RA resistant PLZF-RARA murine APL [12]. We found that the NeuRA1 and NeuRA2 clusters highly expressed a computed PML-RARA RA-responsive signature confirming that the two clusters were composed of RA-responsive blasts (**Figure 1G**). By contrast, the ReP cluster highly or specifically expressed the proliferative E2F signature (**Figure 1H**), and the deubiquitinase *Usp37* involved in PLZF-RARA fusion stability [15] (**Figure 1I**). E2F and *Usp37* expressions persisted upon RA treatment likely supporting the malignancy and RA insensitivity of these cells (**Figure S1H**).

We attempted to purify the ReP cluster after RA treatment based on the expression of specific surface markers identified in our scRNA-seq dataset. Taking into account Cd48 and Itgam (Cd11b), we were limited to isolate Prom1-3 and ReP (ProReP) from NeuRA1 and NeuRA2 (NeuRA) cells (**Figures 1J & S1I**). After RA treatment, whereas the PLZF-RARA fusion was neither detected in the bulk nor in NeuRA populations, ProReP cells did maintain PLZF-RARA expression (**Figures 1K & S1J**) and kept the potential to develop leukemia in transplanted mice (**Figure 1L**).

Altogether, these results reveal transcriptional heterogeneity and differentiation states within the PLZF-RARA transformed cells and identify the ReP cluster, which exhibits no differentiation

features, high E2F signature and PLZF-RARA residual expression as the potential driver of RA resistance of PLZF-RARA leukemia.

Single-cell integrative multi-omics analysis highlights chromatin genes as responsible for RA resistance in PLZF-RARA expressing cells.

To characterize at the regulatory/epigenomic level the heterogeneity underlying PLZF-RARA transformation and RA response, we generated a chromatin accessibility profile (sc-ATACseq) of untreated and RA-treated cells in our PLZF-RARA TG mouse model. To link transcriptome variations with changes in epigenome, we defined a new low-dimensional shared space by mapping cells from our scATAC-seq data to the six scRNA-seq defined clusters [16] (**Figures 2A-B, S2A**). We showed an overall good concordance between the two levels of information (scATAC-seq and scRNA-seq), especially high on RA-treated promyelocytes (**Figures 2A-B)**, confirming the known effect of RA on differentiation through remodeling of chromatin landscape [17]. Interestingly, untreated ReP cells differed from other cells in their chromatin state, including more closed sites. This suggests that in addition to transcriptional reprogramming, epigenetic alterations may predispose the cells to resist to RA (**Figure 2C**). Besides, consistent with our scRNA-seq data, RA-treatment had low impact on the ratio of scATAC-seq cells in the ReP cluster (7% in both conditions) (**Figure 2B**) and on chromatin opening (**Figure 2D**), confirming the little impact of RA on the ReP cluster at both RNA and chromatin levels.

To decipher specific TF activity that might be associated with RA resistance, we inferred information from ATAC-seq and RNA-seq data in the ReP cells (**Figure 2E).** Doing so and in line with our previous annotation, we identified 3 TFs, linked to E2F (E2F1, E2F4, TFDP1) with high transcriptional activity (**Figures 2F, S2B-C).** We performed clustering on their 176 shared targets and highlighted five clusters of genes (**Figure 2G, Table S3**) with a stronger average ATAC signal at enhancer regions than at promoters. Two clusters of genes (Cl_4 and Cl_5) were highly expressed in comparison to the others and not impacted by RA treatment. These genes were not highly expressed but modified by RA treatment in the RA-responsive NeuRA2 cells (**Figure S2D, Table S3**) suggesting a role of these genes in RA resistance. In line with our previous analysis, these highly expressed genes (*Pcna, Mcm2-7 and Ezh2*) were related to DNA repair, replication and chromatin.

The results show that RA resistance depends on E2F transcriptional activity and relies on differences in chromatin accessibility, mainly at enhancer regions.

EZH2 is necessary for PLZF-RARA transformation activity

EZH2 is a component of PRC2 whose canonical enzymatic activity induces the repressive histone mark H3K27me3, frequently involved in AML [18]. To ascertain the functional relevance of EZH2 in PLZF-RARA APL cells, we first confirmed its high expression in the ReP cluster and after RA-treatment (**Figure 3A**), and the presence of E2F1, E2F4 and TFDP1 binding motifs in its promoter (**Figure 3B**). Next, we analyzed the clonogenic activity of PLZF-RARA in the absence of EZH2 *ex vivo* by transducing bone marrow (BM) lineage negative cells of a conditional KO *Ezh2* mouse model [19] with a *PLZF-RARA-IRES-GFP* retroviral construct and performing replating assay (**Figure 3C**). Consistent with our single cell data, PLZF-RARA transduction in lineage-negative cells induced, as soon as the second plating, an overall increase in both EZH2 and H3K27me3 levels (**Figure 3D**) while sustaining replatings (**Figure S3A**). *Ezh2* deletion (Δ/Δ), even in the absence of RA, reduced the cell number and dramatically altered the replating capacity of the PLZF-RARA expressing cells (**Figure 3E**) and promoted their terminal differentiation (**Figure 3F**). *Ezh2* deletion and the consecutive H3K27me3 loss were associated with a PLZF-RARA decrease (**Figure 3D & S3B**) which was consistent with the altered replating capacity. This loss in replating capacity was also observed when *Ezh2* deletion was achieved *in vivo* before PLZF-RARA transduction (**Figure S3C)** or *ex vivo* after the transformation process (**Figure S3D**). Finally, we showed that knocking down (KD) EZH2 in PLZF-RARA-TG BM, decreased PLZF-RARA expression, significantly delayed the development of leukemia and prolonged the survival of the transplanted mice (**Figures 3G & S3E**). These assays suggest that EZH2 is required for the initiation and maintenance of PLZF-RARA oncogenic activity.

We next investigated a potential interaction between the PLZF-RARA fusion protein and EZH2 using a myeloid cell line inducible for PLZF-RARA (U937-B412) (**Figure 3H**) and HEK293T cells overexpressing a Flag-tagged EZH2 and PLZF-RARA (**Figure S3F**). In both systems, we could not demonstrate any interaction between PLZF-RARA and EZH2 or SUZ12, another PRC2 component. However, we evidenced a stronger interaction between EZH2 and SUZ12 in the presence of PLZF-RARA than without (**Figure 3H).** The increase in interaction was not found in the presence of PML-RARA, demonstrating a specificity of the stabilizing effect of PLZF-RARA on the EZH2/SUZ12 complex. To test whether the E2F-EZH2 axis was involved in RA signaling, we KD EZH2 or E2F1 and quantified RA response by using a reporter luciferase assay under a RARE element. We showed that reduction of either EZH2 or E2F1 increased the RA response in the absence of PLZF-RARA but had no impact on PLZF-RARA repression activity (**Figure 3I**), suggesting that EZH2 *per se* limits signaling to RA.

Collectively, these results reveal a dependence of leukemic cells expressing PLZF-RARA on EZH2, whose activity may itself be modified by the presence of the fusion protein.

PLZF-RARA induced H3K27me3 level at specific enhancers genes that marks RA relapse initiating cells

Next, we investigated the effect of PLZF-RARA expression on EZH2 chromatin activity. We compared the epigenetic landscape of PLZF-RARA promyelocytes with the Granulocyte-Monocyte-Progenitor (GMP) compartment (public dataset GSE124190) [20], which is the closest cell compartment to promyelocytes according to its transcriptional signature (**Figure S4A**). Because our scATAC-seq data revealed stronger chromatin opening at enhancer than promoter regions (**Figure 2G**) and since cis-regulatory enhancer elements are known to influence the development of leukemia [21], we mapped the four histone marks (H3K27ac, H3K27me3, H3K4me1 and H3K4me3) that allow to discriminate active (H3K27ac-enriched) and poised (H3K27me3-enriched) enhancers [20] (**Figure S4B**). By comparing PLZF-RARA promyelocytes with GMP genomic enhancer distribution, we found that PLZF-RARA expression modified poised (H3K27me3-enriched) enhancer distributions (68% of them were specific to PLZF-RARA condition) or active (H3K27ac-enriched) enhancer (30% of them were specific to PLZF-RARA condition) distributions (**Figure 4A**). We decided to focus on the new poised enhancers as they reflected a functional difference in H3K27me3 enrichment shifting from enhancers regulating developmental processes to those regulating kinase signaling and bloodstream systems (**Figure S4C**).

Next, we focused on switched enhancers which were marked by H3K27ac in GMP condition but gained H3K27me3 with PLZF-RARA expression (**Figures 4A, S4D**). Although these switched enhancers were in the minority (175 of a total of 3,876 PLZF-RARA induced poised enhancers), they exerted a specific effect on the expression of their nearby genes in the ReP cluster, in which the expression was lower compared with the other clusters (**Figure 4B, upper panel**). In contrast*, de novo* enhancer-associated genes were equally weakly expressed in all scRNA-seq clusters (**Figure 4B, lower panel**). Gene Ontology (GO) analysis revealed that switched enhancer-related genes were associated with myeloid cell differentiation and pro-apoptotic terms (**Figure 4C**). In addition, their expression was decreased in the presence of PLZF-RARA (**Figure S4E**). This indicates that PLZF-RARA expression resulted in a redistribution of repressed enhancers that may be related to RA unresponsiveness.

To determine the role of EZH2 in RA resistance, we investigated the effect of RA on EZH2 chromatin activity after sequential transplantations (**Figure 4D**). In line with the literature [11], RA treatment, although inducing a clear differentiation of blasts (**Figure 4E, upper panel**), did not eradicate relapse-initiating cells, since relapse was observed at day 17 post-transplant in mice transplanted with RA-treated BMs (**Figure 4E, lower panel**). RA treatment decreased the overall

level of H3K27me3 as early as day 3 of treatment (**Figure 4F**), while increasing EZH2 protein level, which was consistent with our scRNA-seq data (**Figure 3A**). Interestingly, leukemia relapse of RA-treated BM was characterized with a restoration of high H3K27me3 levels in the leukemic cells (**Figure 4F**). This shows that RA had a contrasting effect on EZH2 and suggests that RA-induced differentiated cells maintained EZH2 independently of its methyltransferase activity. More precisely, RA decreased H3K27me3 signal at poised enhancers (**Figure 4G**) and the numbers of these enhancers after 7 days of treatment (**Figure 4H**). Clearly, leukemia relapse was characterized by both the restoration of high levels of H3K27me3 at the enhancer regions and the high number of H3K27me3-enriched enhancers (**Figures 4G-H**). Because PLZF-RARA cells respond differently to RA and the ReP cluster may be responsible for RA resistance, we measured the levels of H3K27me3/H3K27ac after RA treatment and at relapse at the 175 switched enhancers (described in **Figure 4A**). We found that neither RA treatment (3 or 7 days) nor the following transplantations erased H3K27me3 levels or restores H3K27ac signal at these enhancers (**Figures 4I & S5A**). Consistently, the signature of the switched enhancers was not impacted by RA in our scRNA-seq data (**Figure S5B**).

Collectively, these results show that PLZF-RARA modifies EZH2 activity by redirecting the H3K27me3 on a subset of enhancers which are not affected by RA treatment. We also highlighted a discrepancy between EZH2 protein level and its methyltransferase activity during RA-induced differentiation.

Elimination of EZH2 eradicates relapse leukemia initiating cells

Because EZH2 is necessary for PLZF-RARA-induced transformation and high H3K27me3 level at specific loci is a marker of resistance, we questioned the pertinence of targeting EZH2 with GSK126, a S-adenosyl-methionine competitor that inhibits EZH2 methyltransferase activity [22], in combination with RA to overcome resistance. To test this hypothesis, we treated PLZF-RARA TG transplanted mice with GSK126 and/or with RA and transplanted the treated BMs into new recipients to follow disease progression according to the pre-treatment (**Figure 5A**). At first, the inhibitory effect of GSK126 on H3K27me3 level in the treated BM, which was more pronounced when the drug was administered in combination with RA, was confirmed (**Figure 5B**). However, GSK126 treatment did not affect PLZF-RARA protein level (**Figure 5B**) nor the % of PLZF-RARA TG cells (% of Cd45.2 positive cells) in total BM and, in contrast to RA, had no impact on disease progression and blast differentiation, and no synergistic effect of GSK126 with RA was observed (**Figures 5C, left panel & S6A**). At day 13 post-secondary transplantation (**Figure 5C, middle panel**), GSK126-treated BM expanded as untreated BM suggesting that GSK126 alone did not

impact the relapse initiating cells. A delay in leukemia progression was observed in the RA-treated BM, but addition of the GSK126 did not change in any instance the leukemia progression (**Figure 5C, right panel**). To rule out accessibility and dosage problems that could be faced using animal models, we compared the effect of GSK126 alone or in combination with RA on PLZF-RARA replating capacity (**Figure S6B, left panel**). As for the *in vivo* experiment, GSK126 alone or in combination with RA had no effect on the replating capacity of PLZF-RARA *ex vivo* (**Figure S6B, right panel**). These data showed that despite a strong dependency of PLZF-RARA cell transformation on EZH2, inhibition of its catalytic activity is not sufficient to promote APL clearance and further suggested that PLZF-RARA APL depends on a non-canonical activity of EZH2. To explore this possibility, we took advantage of a new commercially available EZH2 degrader, MS1943 (MS) [23]. PLZF-RARA TG BM was treated with MS and/or RA and re-transplanted in new recipient mice (**Figure 5D**). Concomitant with its ability to degrade EZH2, MS effectively erased the global level of H3K27me3 (**Figure S6C**), decreased PLZF-RARA expression at the protein (**Figures 5E & S6C**) and mRNA levels (**Figure S6D**), induced cell differentiation (**Figure 5F**) and reduced cell viability (**Figure 5G**). Despite low synergistic effect of MS with RA *in vitro* (**Figure S6E**), reinjecting alive MS and MS-RA-treated PLZF-RARA BM cells in recipient mice significantly prolonged the survival of the mice, confirming the importance of EZH2 non-canonical activity in PLZF-RARA leukemia development and RA resistance (**Figures 5H & S6F**). To link this loss of leukemic potential upon EZH2 degradation to a transcriptional reprogramming, we performed bulk RNA-seq on PLZF-RARA TG BM treated with MS or GSK (**Figures 5I & S6G, Table S4**). MS treatment was associated with a more pronounced and specific decrease in the expression of ReP cluster marker genes in comparison to GSK treatment (**Figure 5I**). Gene ontology analysis on genes modified by MS further confirmed the importance to degrade EZH2 to target the biological processes (cell cycle and DNA-dependent DNA replication) associated with RA resistance (**Figure S6G**). Interestingly, the gene signature resulting from the targeting of methyltransferase activity of EZH2 (named methyl. targeting) as well as the ReP marker genes were positively correlated to PLZF-RARA patients while genes associated with the targeting of EZH2 non-methyltransferase activity (named Non methyl. targeting) and the NeuRA marker genes were correlated to PML-RARA patients (**Figure 5J**). These data not only show that our RA (un)-response signatures identified in our mouse model could be used for APL patients; they also confirm that targeting EZH2 non-methyltransferase activities is necessary to promote RA sensitivity in APL patients.

Altogether, these results demonstrate that targeting EZH2 methyltransferase activity is not sufficient to eradicate relapse leukemia initiating cells and suggest elimination of EZH2 to overcome RA resistance.

DISCUSSION

Here, we focused on the effect of RA-treatment in APL cells expressing PLZF-RARA, to address leukemic cell heterogeneity and its consequence on therapy resistance. The unique differentiating properties of RA make it a promising drug for the treatment of non-APL AML [24] and solid tumors [25] and a better understanding of resistance mechanisms could widen its use.

Clonal diversity and evolution patterns of AML by high-throughput single-cell genomics (scRNA-seq and scDNA-seq) have revealed hierarchies in the AML with heterogeneity correlating with their underlying genetic alterations[26; 27]. Here, we analyzed the effect of a single oncogenic event and identified different subgroups of PLZF-RARA transformed promyelocytes, which reflect the APL hierarchy as well as spontaneous differentiation. Among them, we identified a cell subgroup, named ReP, which remained transcriptionally and at the chromatin level unperturbed by RA and retained leukemic activity. What could make the Rep cells the RA-resistant cells? The first striking observation, was that this group of cells maintains PLZF-RARA expression after RA treatment, which is known to act as a competitive transcriptional repressor of RARA[28] and block RA signalization [29]. This suggest that in our experimental setting as it was shown for PML-RARA model [8], maintaining PLZF-RARA expression is key for RA-resistance. This also suggests that RA-resistance is not acquired by RA-treatment but inherent to this particular group of transformed promyelocytes. Thus, mechanism of resistance maybe different than the acquired RA resistance observed in PML-RARA patients, which has been associated to additional oncogenic events [30; 31; 32]. These transformed promyelocytes were different from the others with a marked replication/repair program and high E2F activity, which oncogenic activity [33] may support the RA resistance of the cells considering its role in promoting leukemic cell survival [34], escape from apoptosis [35] and resistance to cisplatin treatment [36]. In addition, by inferring our scATAC-seq data we specifically probe the activity of E2F in RA-resistant cells and identify an E2F oncogenic regulatory network involving the PRC2 methyltransferase EZH2. Deregulations of EZH2 are linked to cancer initiation, metastasis, immunity, metabolism and drug resistance in a wide variety of cancer [37] and may contribute to RA-resistance. Thus, although we cannot determine whether the maintenance of PLZF-RARA is the cause or consequence of RA unresponsiveness, we revealed a E2F/EZH2 axis, which can be the key to overcome RA resistance

EZH2 represents one of the most promising epigenetic anticancer therapeutic targets, although its mechanism of action is incompletely understood [38]. Indeed, due to its tissue and mode of action complexity [18] targeting EZH2 in leukemia is challenging. Within the AML entity, EZH2 exerts an oncogenic function by enhancing differentiation blockade during AML maintenance [39], while it acts as a tumor suppressor during leukemia initiation [40]. Here, we demonstrated the dependence of PLZF-RARA leukemia on EZH2 activity, suggesting an oncogenic role of EZH2 in this type of leukemia. However, we clearly showed little effect of inhibiting its methyltransferase activity on PLZF-RARA leukemia progression and relapse, and we demonstrated the need to deplete EZH2 to clear leukemia. This means that PLZF-RARA leukemic cells depend on an oncogenic activity that goes beyond EZH2 catalytic activity.

Molecularly, we showed that PLZF-RARA redirects EZH2 methyltransferase activity on a subset of apoptotic genes and that this PLZF-RARA H3K27me3 induced-signature marks the RA-persistent cells. Interestingly, we could not evidence a direct interaction between EZH2 and PLZF-RARA as we previously did for PLZF [41]. However, we clearly evidenced a stronger association of EZH2 and SUZ12 upon PLZF-RARA induction. This PRC2 stabilization, could either account for a modification of the methyltransferase activity of EZH2 [42; 43] or favor its non-canonical activity [44]. Decreasing EZH2 did not alter the repressive activity of PLZF-RARA although it was able to increase the RARA response, in agreement with the literature showing that EZH2, as part of the PRC2 complex, inhibits RARA signaling during development [45; 46]. Many cancers have been shown to rely on an EZH2 oncogenic effect that is not solely based on its histone transferase activity. This is the case of estrogen receptor (ER)-negative basal-like breast cancers [47], AR dependent prostate cancers [48] [43] or SWI/SNF mutant tumors that rely on both the catalytic and non-catalytic activities of EZH2 [44]. Interestingly, for the latter tumors, as in PLZF-RARA leukemic cells, GSK126 has shown only limited efficacy [44].

By leveraging our own single-cell data, we reveal a novel mechanism of resistance, involving the multifaceted enzyme EZH2, opening up a therapeutic opportunity. We provide evidences by using an EZH2-selective degrader [23], which significantly reduced the growth of PLZF-RARA expressing leukemia cells and increased the survival of transplanted mice of the importance of eliminating the target on which the tumor depends. Our study supports the development of EZH2-Based PROTACs to degrade the PRC2 complex, which targets the enzymatic and non-enzymatic activities of EZH2 [49] and holds great promise for the future treatment of cancers dependent on the non-catalytic activity of EZH2. A very recent study clearly demonstrated that EZH2 depletion inhibits neuroblastoma and small cell carcinoma tumor formation by potentiating MYC degradation [50]. In addition, while revising this work a study came out showing that a

PROTAC EZH2, which degrades almost more efficiently its oncogenic partner MYC is efficient in reducing MLL positive leukemia [51].

In conclusion, we demonstrated the power of single-cell multi-omics to understand cancer cell heterogeneity, to identify treatment-resistant cells and characterize their activity. We also revealed a novel mechanism of RA-resistance dependent on EZH2 non-catalytic activity, which should be considered when developing targeted therapeutic approaches.

RESOURCE AVAILABILITY

Data availability

The raw ChIP-seq, scATAC-seq and scRNA-seq data (fastq files) are deposited under the accession number GSE181190. The repository also contains the bigwig, the peak matrix and the count matrix for the ChIP-seq, scATAC-seq and scRNA-seq respectively. All R and python codes used for data analysis are integrated in a global snakemake workflow available at https://gitcrcm.marseille.inserm.fr/herault/GMP_PRARA.

ACKNOWLEDGMENTS

We thank Dr. Pier Pandolfi for sharing the PLZF-RARA TG mouse model; Dr Valerie. Lallemand-Breitenbach for facilitating the access to the PLZF-RARA TG bone marrow; Dr Christophe Lachaud for helpful discussion and for reading the manuscript and members of the Duprez laboratory for helpful discussions. The authors wish to thank the animal support facility of the Centre de Recherche en Cancérologie de Marseille, the flow cytometry and cell sorting platform, the CIBI and DISC platforms for computational analyses and support.

FUNDING

This work was supported by the Ligue Nationale contre le Cancer (E.D.), the Association Laurette Fugain (E.D.), the Fondation Recherche Médicale (E.D.), the Fondation A*MIDEX (E.D.), the Fondation de France (M.P.), l'Institut National du Cancer grant # 20141PLBIO-06-1 (M.P. and E.D.), the Japan Society for the Promotion of Sciences (JSPS) (M.P.), the Cancéropôle Provence Alpes Côte d'Azur (M.P.), L.H. was supported by a PhD grant from Aix Marseille University. The study was supported by the collaborative IMSUT joint grant between A.I. and E.D. This study was supported partly by a Grant from International Joint Usage/Research Center, The Institute of Medical Science, The University of Tokyo.

AUTHOR DISCLOSURE

The authors declare no conflict of interest

AUTHOR CONTRIBUTIONS

M.P. and E.D. developed the original hypothesis and designed experiments. M.P. with the help from N.P., K.S., W.K., L.N., L.Ha., Y.N.T., M.O. and N.C. performed experiments and/or analyzed data. A.M and L.Hé. carried out computational analyses of the scRNA-seq and scATAC-seq. L.Hé. developed the pipeline for scRNA-seq and scATAC-seq data integration. M.P. and J.V. conducted ChIP-seq analyses. J.V. analyzed RNA-seq. A.I. and D.B. provided reagents and discussed results. M.P., E.D. and A.M. designed the figures and M.P. and E.D. wrote the manuscript. All co-authors proofread the manuscript.

Figure 1: Single-cell transcriptome analysis identifies a subset of retinoic acid resistant PLZF-RARA leukemic cells with a specific signature. (**A**-**B**) UMAP visualization of the scRNA-seq dataset colored by (**A**) condition (NT and RA d7) and by (**B**) cluster (total integrated cells: 11,900). Six clusters were identified: ReP, DNA repair/Replication/Proliferation; Prom1-3, Neutrophil 1-3; NeuRA1-2, Neutrophil Retinoic Acid 1-2. (**C**) Lower panel: NT and RA cell distribution in each cluster. The black vertical line indicates expected NT and RA cell proportions according to the dataset size. Upper panel: absolute cell number per cluster and per condition. Names of the clusters for which the proportion of NT or RA cells is significantly higher than expected (p-value < 0.01) are colored in purple for NT cells and in orange for RA cells. (**D**) Differentiation trajectory. On top, schematic representation of the different states (A, B, C, D, E) in each trajectory (Trajectory 1: A-C-D, Trajectory 2: A-C-E, Trajectory 3: A-B). Below, UMAP is colored according to the pseudotime value of each cell. (**E**) Cluster distribution in each state of the pseudotime. (**F**) NT and RA cell distribution (lower: percentage; upper absolute) in each state of the pseudotime. For (**C**) and (**F**) Names of the clusters for which the proportion of NT or RA cells was significantly higher than expected (p-value <0.01) are colored in purple for NT cells and in orange for RA cells. (**G**) Violin plots showing PML-RARA response and (**H**) E2f signature scores in each cluster. For (**G**) and (**H**) The signature score represents the global expression of annotated genes for the selected signature. Gray/black arrows pointing down/up: significant lower/higher expression in the cluster against all the others (average score difference > 0.02 and p-value adjusted < 0.05). (**I**) Violin plot showing *Usp37* expression in each cluster. Black arrows pointing up: significant higher expression in the cluster against all the others (average $\log_2|FC|> 0.1$ and p-value adjusted < 0.05). (**J**) Gating strategy for isolating ProReP cells (Prom1-3 and ReP) and NeuRA (NeuRA1-2). The donut plot represents the proportion of Prom1-3 and ReP cells into the ProReP population according to the scRNA-seq analysis. (**K**) PLZF-RARA (black arrow: full length, black star: degraded form) levels in untreated (NT) and treated promyelocytes (RA d7). Actin is used as loading control. (**L**) Survival

rate of mice transplanted with ProReP or NeuRA cells. Each cohort contains at least 5 mice. *** p-value < 0.001.

Figure 2: Single-cell integrative multi-omics analysis highlights chromatin genes as responsible for RA resistance in PLZF-RARA expressing cells. (**A**) UMAP visualization of integrated scRNA-seq (11,900 cells) and scATAC-seq (7,367 cells) dataset colored by cluster. (**B**) Donut plots showing the distribution of scRNA- and scATAC-seq cells in each cluster for NT and RA d7 conditions. (**C**) Left panel: heatmap showing the ATAC signal in the NT condition on the differentially accessible peaks between ReP and Prom2-3 clusters. Hierarchical clustering is done according to the ReP dataset. Right panel: coverage plot of ATAC signal at selected genes. (**D**) Coverage Plot of ATAC signal per condition in each cluster associated with *Ipcef1*, *Sox6* and *Prdx6b* genes. (**E**) Computational scheme to identify key regulon targets in the ReP cluster. The first filtering consists to select TFs with high activity in the ReP cluster by considering the accessibility of their DNA motifs in this cluster. TF motif accessibility scores are calculated with Signac [52] and TF motif markers are identified for each cluster (**Table S2A**). Selected ReP TFs are cross-referenced with master transcriptional regulators identified from scRNA-seq data using SCENIC [53] (**Table S2B**). After this filtering, 3 TFs remain. Target genes shared at least by 2 TFs are taken into account for further filtering (2nd filtering). Target genes considered are: (i) found in all pySCENIC run, (ii) linked with positive regulons and (iii) filtered based on the sum of normalized importance (> 0.35). 176 genes are conserved (Table S3). (**F**) Boxplots showing E2f1, E2f4 and Tfdp1 (TFs obtained after the 1st filtering) regulon activity in each cluster. * p-value < 0.05 (**G**) Heatmap showing the mRNA expression (left), the promoter accessibility (middle, $\pm$ 3kb from the TSS) and the enhancer accessibility (right, ± 50kb from the TSS minus the ± 3kb promoter region) of the 176 target genes in the ReP cluster (obtained after the 2nd Filtering). Results are expressed as normalized log (mean gene activity). Hierarchical clustering is done according to the NT dataset.

Figure 3: EZH2 relevance in PLZF-RARA APL (**A**) Violin Plot showing *Ezh2* expression per cluster (upper panel) and in NT or RA treated cell conditions per cluster (lower panel). The black arrow pointing up indicate significant higher expression in the cluster against all the other clusters (average $\log_2|FC| > 0.25$ and p-value adjusted < 0.05). (**B**) Coverage Plot of ATAC signal on *Ezh2* gene in the ReP cluster. E2f1, E2f4 and Tfdp1 motifs are detected under the highlighted peak. (**C**) Experimental scheme to ascertain whether Ezh2 activity is required for PLZF-RARA transformation. Lineage negative (Lin$^-$) cells purified from *Cre-ERT;Ezh2$^{fl/fl}$* are purified and transduced with an *empty-IRES-GFP* (IRES) or a *PLZF-RARA-IRES-GFP* (P-RARA) retroviral construct. Lin$^-$ GFP positive cells are purified by FACS and *Ezh2* deletion in Lin- GFP positive cells is obtained by adding 150nM 4-OHT in the methylcellulose. (**D**) Left panel: global levels of PLZF-

RARA (black arrow: full length, black star: degraded form), Ezh2 and H3K27me3 detected by western blotting after 4-OHT-induced Ezh2 deletion in the 2nd round of plating. Actin and H3 are used as loading controls. Right panel: bar plots representing the signal intensity of PLZF-RARA (P-RARA), EZH2 and H3K27me3 normalized to the loading control (for P-RARA) and to the IRES condition (for EZH2 and H3K27me3). ns: not significant; * p-value < 0.05 (two replicates). (**E**) Replating efficiency is monitored by counting the total Colony Forming Units (CFU) of non-transformed (IRES) and PLZF-RARA transformed (P-RARA) cells in presence (*fl/fl*) or absence (*Δ/Δ)* of *Ezh2.* Results are expressed as a mean SD of three experiments (n=3). *p-value < 0.05, ns: not significant. (**F**) Cell morphology of P-RARA or IRES-transduced cells in presence (*fl/fl*) or absence (*Δ/Δ)* of *Ezh2.* Representative colonies of indicated conditions after 2 rounds of plating. Cells are cytospun and observed after May-Grünwald Giemsa (MGG) staining; magnification 64X; bar 10 µm. (**G**) Left panel: experimental scheme to ascertain whether Ezh2 activity is required for PLZF-RARA leukemia development *in vivo*. PLZF-RARA TG BM is transduced with a shCtrl-GFP or a shEZH2-GFP retroviral construct. GFP positive cells are purified by FACS and reinjected into recipient mice. Right panel: survival rate of mice transplanted with shCtrl (grey curve) or shEZH2 cells (green curve). Each cohort contains 5 mice. *** p-value < 0.001 (**H**) Nuclear extracts of U937 cells treated or not with ZnSO4 (Zn) immunoprecipitated with anti-IgG, anti-EZH2 or anti-SUZ12 antibodies. IPs are immunoblotted with anti-PLZF (upper panel) or anti-EZH2 antibodies (lower panel). Inputs (in) represent 2% of samples processed in each IP. U937 B412: PLZF-RARA Zn-inducible; U937 MT: parental cells; U937 PR9: PML-RARA Zn-inducible. (**I**) Relative Luciferase intensity (AU: Arbitrary Units) monitored in HEK293T transduced or not (NT) with a shEZH2 (left panel) or transfected with a siE2F1 or siCtrl (NT) (right panel). Cells were transfected with the RARE-Luc and with a GFP (ᔓ P-RARA) or PLZF-RARA (P-RARA) construct. Cells are treated or not for 48 hours with retinoic acid (RA, 1µM). ns: not significant; * p-value < 0.05, ** p-value < 0.01 (n=6).

Figure 4: PLZF-RARA induced H3K27me3 level at specific enhancers genes that marks RA relapse initiating cells. (**A**) Enhancer distribution in PLZF-RARA promyelocytes and normal GMPs. Overlap of Active (left panel) and Poised enhancers (right panel) in GMP and PLZF-RARA (P-RARA) conditions. *** p-value < 0.001. The poised enhancer dynamics upon PLZF-RARA expression is schematized below. Triangles represent enhancers; colors indicate their activity (active: blue, poised: red). Empty triangles: no change in enhancer activity between the two conditions. (**B**) Violin plots showing "switched" and "*de novo*" Poised signature scores per cluster. Signature score represents the global expression of annotated genes for the signature identified by scRNA-seq. Grey arrow pointing down: significant lower expression in the cluster against all the others

(average score difference > 0.005 and p-value adjusted < 0.05). (**C**) GO analysis of enhancer nearby genes. Gene %: number of genes observed/total number of genes within each GO term. (**D**) Experimental scheme to assess chromatin events associated with RA resistance. PLZF-RARA TG BM is transplanted into recipient mice. Ten days after, mice are injected with corn oil (NT) or with RA for 3 or 7 days (d3 and d7) and sacrificed. Treated BMs are immunophenotyped and reinjected into new recipient mice (tNT, td3, td7). Secondary transplanted mice are not treated (Ø) and sacrificed at day 17 post-transplantation. (**E**) Leukemia evolution analyzed by MGG staining (magnification 64X), spleen size (bar in centimeter) and FACS (Cd45.2, Cd11b and Gr1 are monitored). Upper panel: impact of RA on PLZF-RARA leukemia (NT, d3, d7). Lower panel: leukemia relapse evaluation of transplanted untreated (tNT) and RA-treated BM (td3, td7). (**F**) Left panel: global levels of PLZF-RARA (black arrow: full length, black star: degraded form), EZH2 and H3K27me3. Actin and H3 are used as loading controls. Signal intensity is normalized according to the loading control and to the NT. Right panel: bar plots representing the signal intensity of PLZF-RARA (P-RARA), EZH2 and H3K27me3 normalized to the loading control and to the NT condition. * p-value < 0.05 (two biological replicates). (**G**) Representative IGV tracks of H3K27me3 in NT, d7 and td7 conditions. The gray box underlines enhancer coordinates. (**H**) Total number of poised enhancers in each condition. (**I**) Plot Heatmap of H3K27ac (blue) and H3K27me3 (red) signals in GMP, NT, d7 and td7 conditions at switched enhancers. Signals are plotted 10Kb and 0.1 Mb up-downstream the enhancer center.

Figure 5: Impact of targeting EZH2 on APL progression. (A) Experimental scheme of the analysis of RA, GSK or combo treated bone marrow. PLZF-RARA TG bone marrow is transplanted into recipient mice. Seven days after, mice are injected for 3 days with GSK126 (GSK) or with corn oil (NT) followed by 7 consecutive days of RA (RA). After treatments (NT: corn oil, GSK, RA, GSK and RA) mice are sacrificed and treated-BM are immunophenotyped and reinjected into new recipient mice (tNT, tGSK, tRA, tGSK+RA). At this time treatments are stopped (Ø). Mice are sacrificed 15-20 days after the secondary transplantation. (**B**) Left panel: global levels of PLZF-RARA (black arrow: full length, black star: degraded form), Ezh2 and H3K27me3. Actin is used as loading control. Right panel: bar plots representing the signal intensity of PLZF-RARA (P-RARA), EZH2 and H3K27me3 normalized to the loading control and to the NT condition. * p-value < 0.05 (three biological replicates). (**C**) Left panel: impact of GSK, RA and combo treatments on PLZF-RARA leukemia at day 17 after the 1st transplantation (NT, GSK, RA, GSK+RA). Middle and right panels: evaluation of leukemia relapse monitored by FACS analysis (Cd45.2, Cd11b and Gr1 markers are monitored) at day 13 (d13) and day 18 (d18) after the secondary transplantation (tNT, tGSK, tRA, tGSK+RA). (**D**) Scheme resuming the protocol to evaluate the effect of MS1943

(MS) treatment on PLZF-RARA BM. (**E**) Left panel: global levels of PLZF-RARA and Ezh2 after RA (0.1µM) and/or MS1943 (MS, 1.25µM) treatments. Actin is used as loading controls. Right panel: bar plots representing the signal intensity of PLZF-RARA (P-RARA) and EZH2 normalized to the loading control and to the NT condition. * p-value < 0.05 (two biological replicates). (**F**) Cell morphology analyzed by MGG staining (magnification 64X; bar 20 µm); (**G**) Cell viability of PLZF-RARA TG cells upon GSK126 (GSK) or MS1943 (MS) treatments monitored by bioluminescence. Results are expressed by percent of living cells and normalized to the untreated condition (NT). results are expressed as the mean SD of three independent experiments (n=3). *p-value < 0.05, *** p-value < 0.001. (**H**) Survival rate of mice transplanted with untreated (tNT, grey curve, 8 mice), GSK126 (tGSK, 2.5µM, blue curve, 5 mice), RA (tRA, 0.1µM, 5 mice), MS1943 (tMS, 2.5µM, purple curve, 10 mice), MS and RA (tMS+RA, 1.25µM MS and 0.1µM RA, green curve, 5 mice) pre-treated PLZF-RARA TG bone marrow. ** p-value < 0.01, * p-value < 0.05. (**I**) RNA-seq (two biological replicates) performed on promyelocytes purified from PLZF-RARA TG mice and treated or not (NT) with MS1943 (MS, 2.5µM) or GSK126 (GSK, 2.5µM) (*in vitro* treatments). Impact of MS1943 (MS) and GSK126 (GSK) on the expression of the most differentially over-expressed genes in the ReP cluster compared to the other clusters. Results are expressed as gene counts z-score. (**J**) Gene set enrichment analysis of t(11;17) APL patients (PLZF-RARA) compared to t(15;17) APL patients (PML-RARA). ReP, NeuRA, the targeting of non-methyltransferase activities of EZH2 (Non methyl.targeting) and the targeting of methyltransferase activities of EZH2 (Methyl. targeting) enrichment signatures (ES) are computed.

REFERENCES

1. Dos Santos GA, Kats L, Pandolfi PP. Synergy against PML-RARa: targeting transcription, proteolysis, differentiation, and self-renewal in acute promyelocytic leukemia. *J Exp Med*. 2013;210(13):2793-2802.
2. Di Croce L. Chromatin modifying activity of leukaemia associated fusion proteins. *Hum Mol Genet*. 2005;14 Spec No 1:R77-84.
3. Grignani F, De Matteis S, Nervi C, et al. Fusion proteins of the retinoic acid receptor-alpha recruit histone deacetylase in promyelocytic leukaemia. *Nature*. 1998;391(6669):815-818.
4. Huang ME, Ye YC, Chen SR, et al. Use of all-trans retinoic acid in the treatment of acute promyelocytic leukemia. *Blood*. 1988;72(2):567-572.
5. de The H, Chen Z. Acute promyelocytic leukaemia: novel insights into the mechanisms of cure. *Nat Rev Cancer*. 2010;10(11):775-783.
6. Jimenez JJ, Chale RS, Abad AC, Schally AV. Acute promyelocytic leukemia (APL): a review of the literature. *Oncotarget*. 2020;11(11):992-1003.
7. Sobas M, Talarn-Forcadell MC, Martinez-Cuadron D, et al. PLZF-RARalpha, NPM1-RARalpha, and Other Acute Promyelocytic Leukemia Variants: The PETHEMA Registry Experience and Systematic Literature Review. *Cancers (Basel)*. 2020;12(5).

8. Nasr R, Guillemin MC, Ferhi O, et al. Eradication of acute promyelocytic leukemia-initiating cells through PML-RARA degradation. *Nat Med*. 2008;14(12):1333-1342.
9. Ablain J, de The H. Retinoic acid signaling in cancer: The parable of acute promyelocytic leukemia. *Int J Cancer*. 2014;135(10):2262-2272.
10. He LZ, Guidez F, Tribioli C, et al. Distinct interactions of PML-RARalpha and PLZF-RARalpha with co- repressors determine differential responses to RA in APL. *Nat Genet*. 1998;18(2):126-135.
11. Boukarabila H, Saurin AJ, Batsche E, et al. The PRC1 Polycomb group complex interacts with PLZF/RARA to mediate leukemic transformation. *Genes Dev*. 2009;23(10):1195-1206.
12. Rego EM, He LZ, Warrell RP, Jr., Wang ZG, Pandolfi PP. Retinoic acid (RA) and As2O3 treatment in transgenic models of acute promyelocytic leukemia (APL) unravel the distinct nature of the leukemogenic process induced by the PML-RARalpha and PLZF-RARalpha oncoproteins. *Proc Natl Acad Sci U S A*. 2000;97(18):10173-10178.
13. Kim KH, Roberts CW. Targeting EZH2 in cancer. *Nat Med*. 2016;22(2):128-134.
14. He LZ, Bhaumik M, Tribioli C, et al. Two critical hits for promyelocytic leukemia. *Mol Cell*. 2000;6(5):1131-1141.
15. Yang WC, Shih HM. The deubiquitinating enzyme USP37 regulates the oncogenic fusion protein PLZF/RARA stability. *Oncogene*. 2013;32(43):5167-5175.
16. Stuart T, Butler A, Hoffman P, et al. Comprehensive Integration of Single-Cell Data. *Cell*. 2019;177(7):1888-1902 e1821.
17. Gudas LJ. Retinoids induce stem cell differentiation via epigenetic changes. *Semin Cell Dev Biol*. 2013;24(10-12):701-705.
18. Lund K, Adams PD, Copland M. EZH2 in normal and malignant hematopoiesis. *Leukemia*. 2014;28(1):44-49.
19. Mochizuki-Kashio M, Mishima Y, Miyagi S, et al. Dependency on the polycomb gene Ezh2 distinguishes fetal from adult hematopoietic stem cells. *Blood*. 2011;118(25):6553-6561.
20. Poplineau M, Vernerey J, Platet N, et al. PLZF limits enhancer activity during hematopoietic progenitor aging. *Nucleic Acids Res*. 2019;47(9):4509-4520.
21. Bhagwat AS, Lu B, Vakoc CR. Enhancer dysfunction in leukemia. *Blood*. 2018;131(16):1795-1804.
22. McCabe MT, Ott HM, Ganji G, et al. EZH2 inhibition as a therapeutic strategy for lymphoma with EZH2-activating mutations. *Nature*. 2012;492(7427):108-112.
23. Ma A, Stratikopoulos E, Park K-S, et al. Discovery of a first-in-class EZH2 selective degrader. *Nature Chemical Biology*. 2020;16(2):214-222.
24. Kahl M, Brioli A, Bens M, et al. The acetyltransferase GCN5 maintains ATRA-resistance in non-APL AML. *Leukemia*. 2019;33(11):2628-2639.
25. Geoffroy MC, Esnault C, de The H. Retinoids in hematology: a timely revival? *Blood*. 2021;137(18):2429-2437.
26. van Galen P, Hovestadt V, Wadsworth Ii MH, et al. Single-Cell RNA-Seq Reveals AML Hierarchies Relevant to Disease Progression and Immunity. *Cell*. 2019;176(6):1265-1281 e1224.
27. Stetson LC, Balasubramanian D, Ribeiro SP, et al. Single cell RNA sequencing of AML initiating cells reveals RNA-based evolution during disease progression. *Leukemia*. 2021.
28. Grignani F, Ferrucci PF, Testa U, et al. The acute promyelocytic leukemia-specific PML-RAR alpha fusion protein inhibits differentiation and promotes survival of myeloid precursor cells. *Cell*. 1993;74(3):423-431.
29. Ruthardt M, Testa U, Nervi C, et al. Opposite effects of the acute promyelocytic leukemia PML-retinoic acid receptor alpha (RAR alpha) and PLZF-RAR alpha fusion proteins on retinoic acid signalling. *Mol Cell Biol*. 1997;17(8):4859-4869.
30. Lehmann-Che J, Bally C, Letouzé E, et al. Dual origin of relapses in retinoic-acid resistant acute promyelocytic leukemia. *Nature Communications*. 2018;9(1):2047.
31. Fasan A, Haferlach C, Perglerova K, Kern W, Haferlach T. Molecular landscape of acute promyelocytic leukemia at diagnosis and relapse. *Haematologica*. 2017;102(6):e222-e224.

32. Iaccarino L, Ottone T, Alfonso V, et al. Mutational landscape of patients with acute promyelocytic leukemia at diagnosis and relapse. *Am J Hematol*. 2019;94(10):1091-1097.
33. Kent LN, Leone G. The broken cycle: E2F dysfunction in cancer. *Nature Reviews Cancer*. 2019;19(6):326-338.
34. Rishi L, Hannon M, Salome M, et al. Regulation of Trib2 by an E2F1-C/EBPalpha feedback loop in AML cell proliferation. *Blood*. 2014;123(15):2389-2400.
35. Wu ZL, Zheng SS, Li ZM, Qiao YY, Aau MY, Yu Q. Polycomb protein EZH2 regulates E2F1-dependent apoptosis through epigenetically modulating Bim expression. *Cell Death Differ*. 2010;17(5):801-810.
36. Folk WP, Kumari A, Iwasaki T, et al. Loss of the tumor suppressor BIN1 enables ATM Ser/Thr kinase activation by the nuclear protein E2F1 and renders cancer cells resistant to cisplatin. *J Biol Chem*. 2019;294(14):5700-5719.
37. Duan R, Du W, Guo W. EZH2: a novel target for cancer treatment. *Journal of Hematology & Oncology*. 2020;13(1):104.
38. Eich ML, Athar M, Ferguson JE, 3rd, Varambally S. EZH2-Targeted Therapies in Cancer: Hype or a Reality. *Cancer Res*. 2020;80(24):5449-5458.
39. Tanaka S, Miyagi S, Sashida G, et al. Ezh2 augments leukemogenicity by reinforcing differentiation blockage in acute myeloid leukemia. *Blood*. 2012;120(5):1107-1117.
40. Basheer F, Giotopoulos G, Meduri E, et al. Contrasting requirements during disease evolution identify EZH2 as a therapeutic target in AML. *J Exp Med*. 2019;216(4):966-981.
41. Koubi M, Poplineau M, Vernerey J, et al. Regulation of the positive transcriptional effect of PLZF through a non-canonical EZH2 activity. *Nucleic Acids Res*. 2018;46(7):3339-3350.
42. Pasini D, Bracken AP, Jensen MR, Lazzerini Denchi E, Helin K. Suz12 is essential for mouse development and for EZH2 histone methyltransferase activity. *The EMBO journal*. 2004;23(20):4061-4071.
43. Margueron R, Reinberg D. The Polycomb complex PRC2 and its mark in life. *Nature*. 2011;469(7330):343-349.
44. Kim KH, Kim W, Howard TP, et al. SWI/SNF-mutant cancers depend on catalytic and non-catalytic activity of EZH2. *Nat Med*. 2015;21(12):1491-1496.
45. Laursen KB, Mongan NP, Zhuang Y, Ng MM, Benoit YD, Gudas LJ. Polycomb recruitment attenuates retinoic acid-induced transcription of the bivalent NR2F1 gene. *Nucleic Acids Res*. 2013;41(13):6430-6443.
46. Thulabandu V, Ferguson JW, Phung M, Atit RP. EZH2 modulates retinoic acid signaling to ensure myotube formation during development. *FEBS Lett*. 2022.
47. Lee ST, Li Z, Wu Z, et al. Context-specific regulation of NF-kappaB target gene expression by EZH2 in breast cancers. *Mol Cell*. 2011;43(5):798-810.
48. Kim J, Lee Y, Lu X, et al. Polycomb- and Methylation-Independent Roles of EZH2 as a Transcription Activator. *Cell Rep*. 2018;25(10):2808-2820 e2804.
49. Liu Z, Hu X, Wang Q, et al. Design and Synthesis of EZH2-Based PROTACs to Degrade the PRC2 Complex for Targeting the Noncatalytic Activity of EZH2. *J Med Chem*. 2021;64(5):2829-2848.
50. Wang L, Chen C, Song Z, et al. EZH2 depletion potentiates MYC degradation inhibiting neuroblastoma and small cell carcinoma tumor formation. *Nature Communications*. 2022;13(1):12.
51. Wang J, Yu X, Gong W, et al. EZH2 noncanonically binds cMyc and p300 through a cryptic transactivation domain to mediate gene activation and promote oncogenesis. *Nat Cell Biol*. 2022;24(3):384-399.
52. Stuart T, Srivastarva A, Lareau C, Satija R. Multimodal single-cell chromatin analysis with Signac. *bioRxiv*. 2020.
53. Aibar S, Gonzalez-Blas CB, Moerman T, et al. SCENIC: single-cell regulatory network inference and clustering. *Nat Methods*. 2017;14(11):1083-1086.

Figure 1

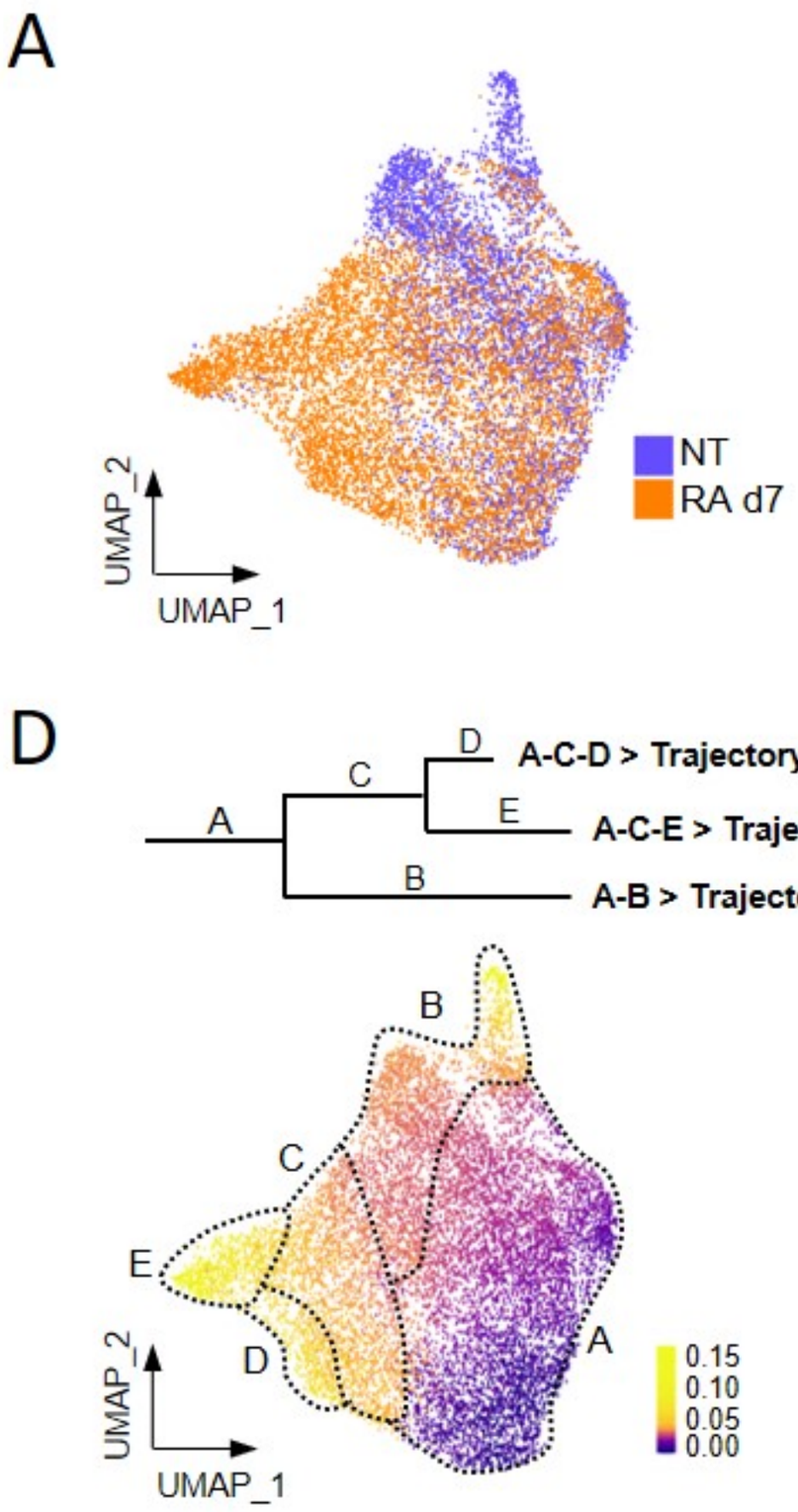
A
UMAP_2
UMAP_1
NT
RA d7
B
Prom2
Prom3
Prom1
NeuRA2
NeuRA1
ReP
UMAP_2
UMAP_1
C
nCells (x10^3)
Sample (%)
NT
RA d7
ReP
Prom1
Prom2
Prom3
NeuRA1
NeuRA2
D
A-C-D > Trajectory 1
A-C-E > Trajectory 2
A-B > Trajectory 3
UMAP_2
UMAP_1
0.15
0.10
0.05
0.00
E
Sample (%)
ReP
Prom1
Prom2
Prom3
NeuRA1
NeuRA2
F
nCells (x10^3)
Sample (%)
NT
RA d7
G
PML-RARA response
Expression level
H
E2F signature
Expression level
I
Usp37
Expression level
J
RA d7
ProReP
3%
39%
NeuRA
Cd48
Cd11b
RNA
39%
43%
13%
ReP
Prom1
Prom2
Prom3
K
NT
RA d7
kDa
Bulk
Bulk
ProReP
NeuRA
110
80
40
P-RARA
ACTIN
L
NeuRA
ProReP
***
Survival (%)
Days

Figure 2

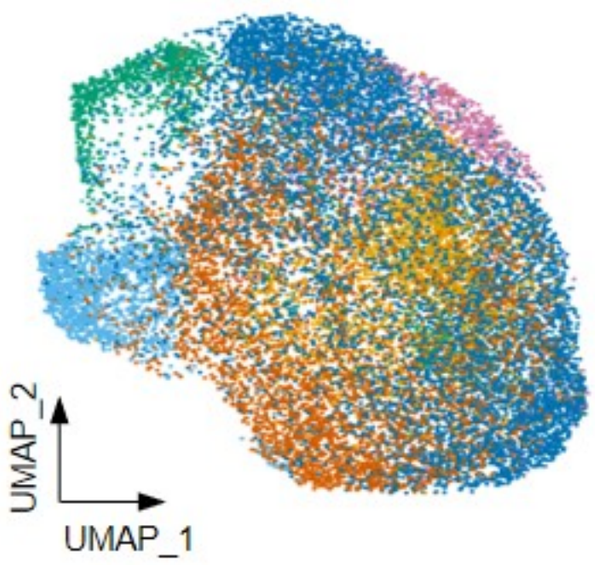
A
UMAP_2
UMAP_1

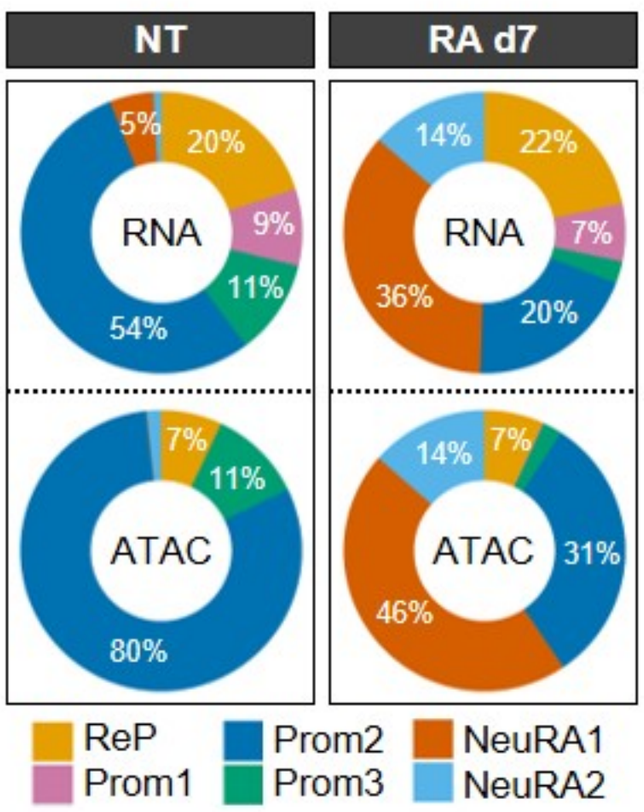
B
NT
RA d7
5%
20%
9%
11%
54%
RNA
14%
22%
7%
36%
20%
RNA
7%
11%
80%
ATAC
14%
7%
31%
46%
ATAC
ReP
Prom1
Prom2
Prom3
NeuRA1
NeuRA2

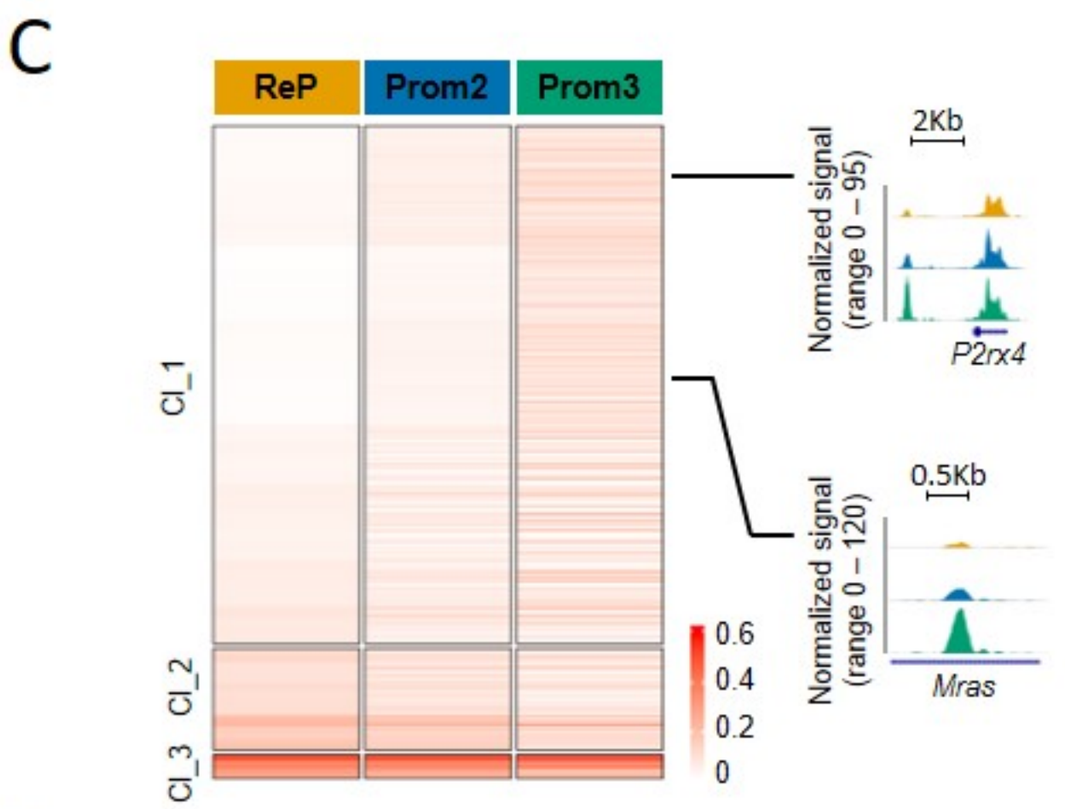
C
ReP
Prom2
Prom3
CI_1
CI_2
CI_3
0.6
0.4
0.2
0
2Kb
Normalized signal (range 0 – 95)
P2rx4
0.5Kb
Normalized signal (range 0 – 120)
Mras

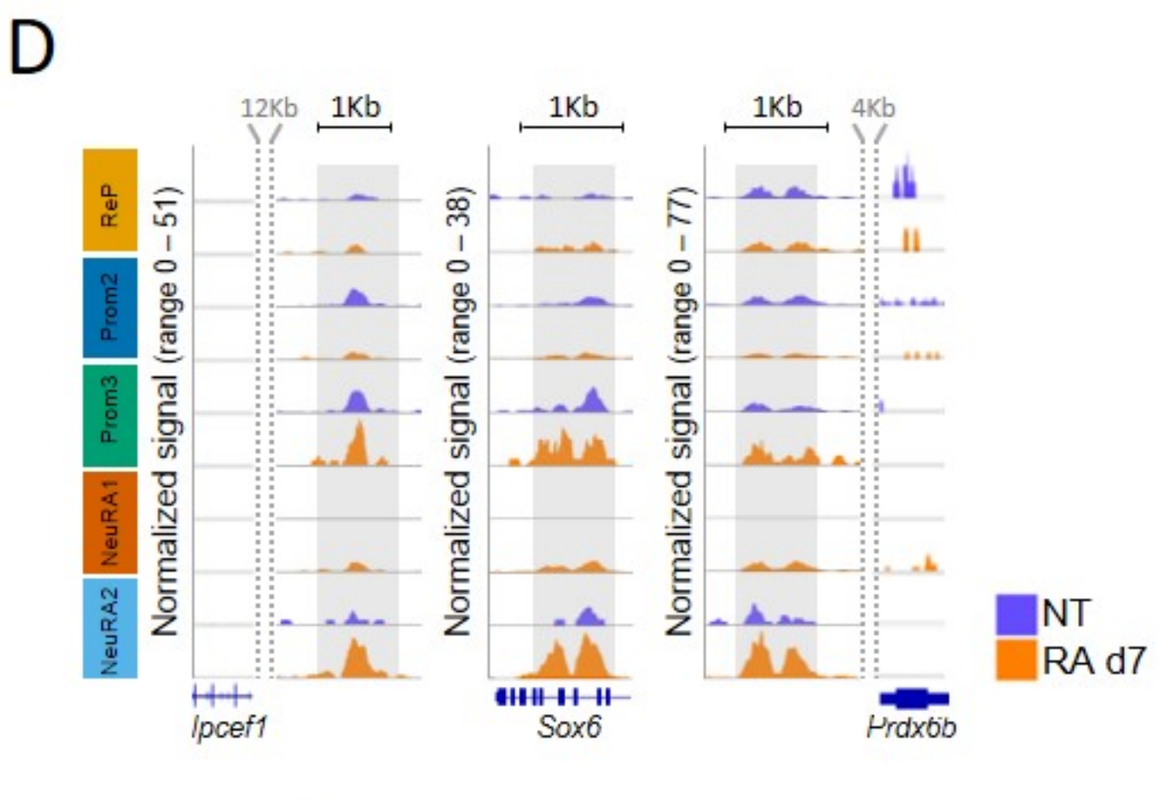
D
12Kb
1Kb
1Kb
1Kb
4Kb
ReP
Prom2
Prom3
NeuRA1
NeuRA2
Normalized signal (range 0 – 51)
Normalized signal (range 0 – 38)
Normalized signal (range 0 – 77)
Ipcef1
Sox6
Prdx6b
NT
RA d7

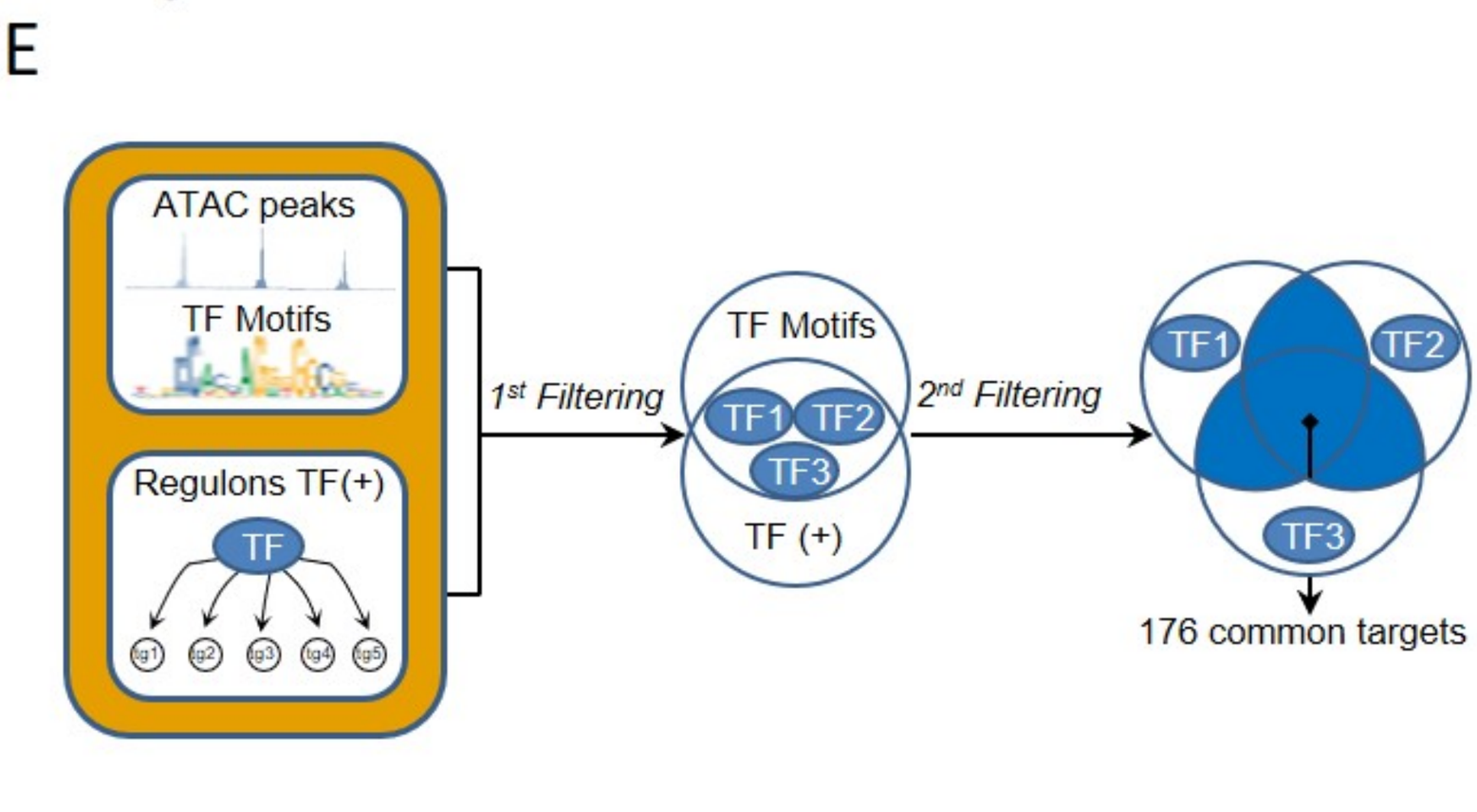
E
ATAC peaks
TF Motifs
Regulons TF(+)
TF
tg1
tg2
tg3
tg4
tg5
1st Filtering
TF Motifs
TF1
TF2
TF3
TF (+)
2nd Filtering
TF1
TF2
TF3
176 common targets

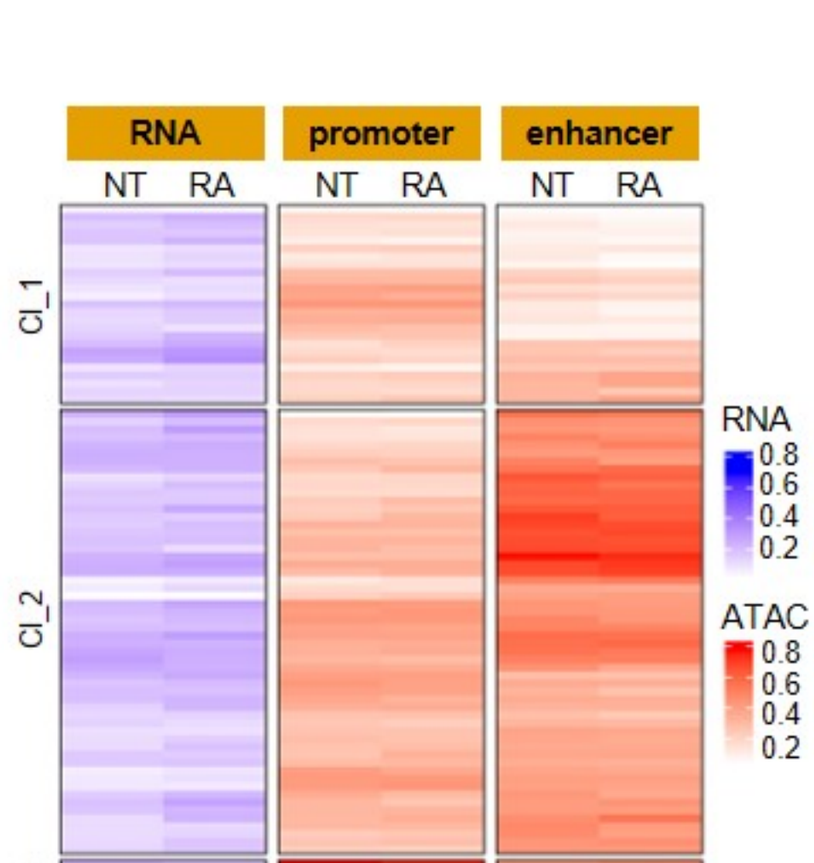
G
RNA
promoter
enhancer
NT
RA
CI_1
CI_2
CI_3
CI_4
CI_5
RNA
0.8
0.6
0.4
0.2
ATAC
0.8
0.6
0.4
0.2
Pcna
Mcm7
Mcm6
Mcm5
Mcm2
Uhrf1
U2af1
Mcm3
Usp1
Mcm4
Ezh2

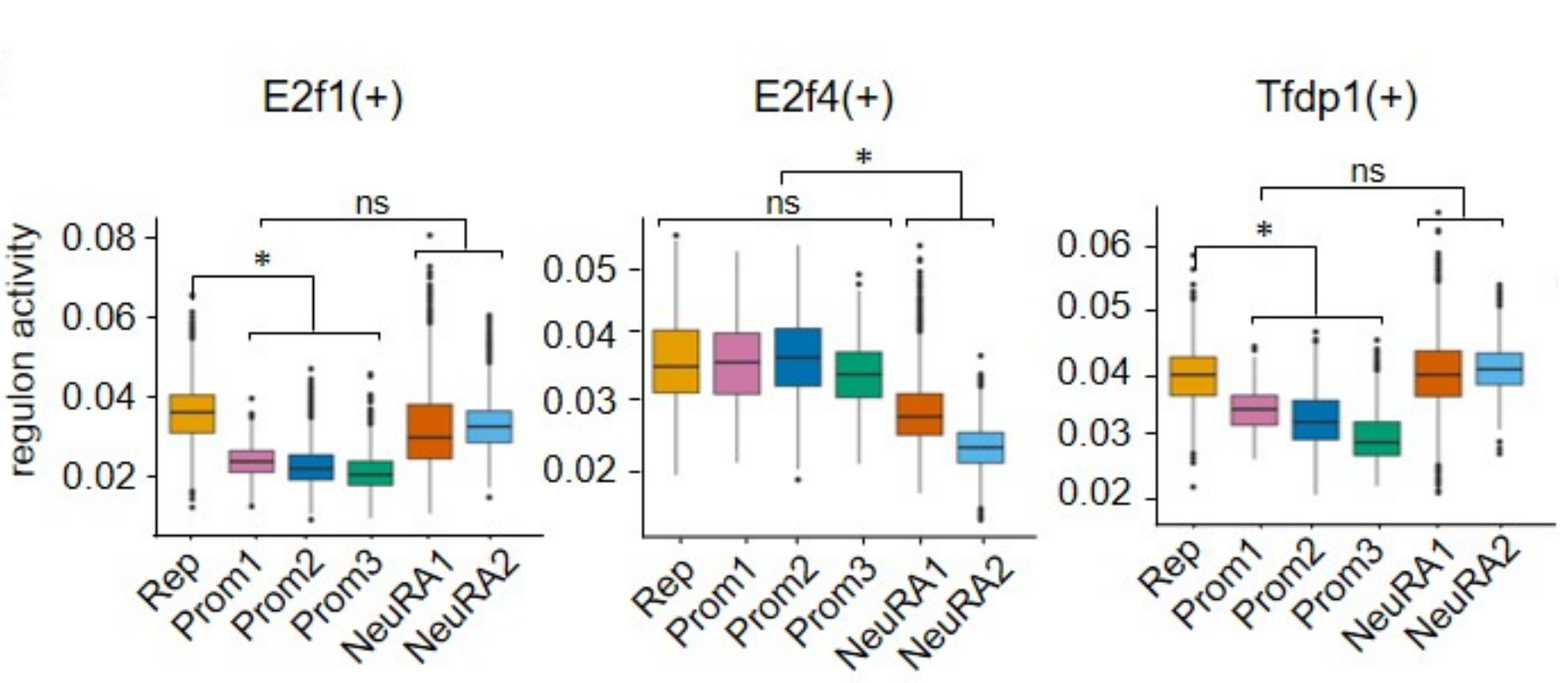
F
E2f1(+)
E2f4(+)
Tfdp1(+)
regulon activity
0.08
0.06
0.04
0.02
0.05
0.04
0.03
0.02
0.06
0.05
0.04
0.03
0.02
ns
*
Rep
Prom1
Prom2
Prom3
NeuRA1
NeuRA2

Figure 3

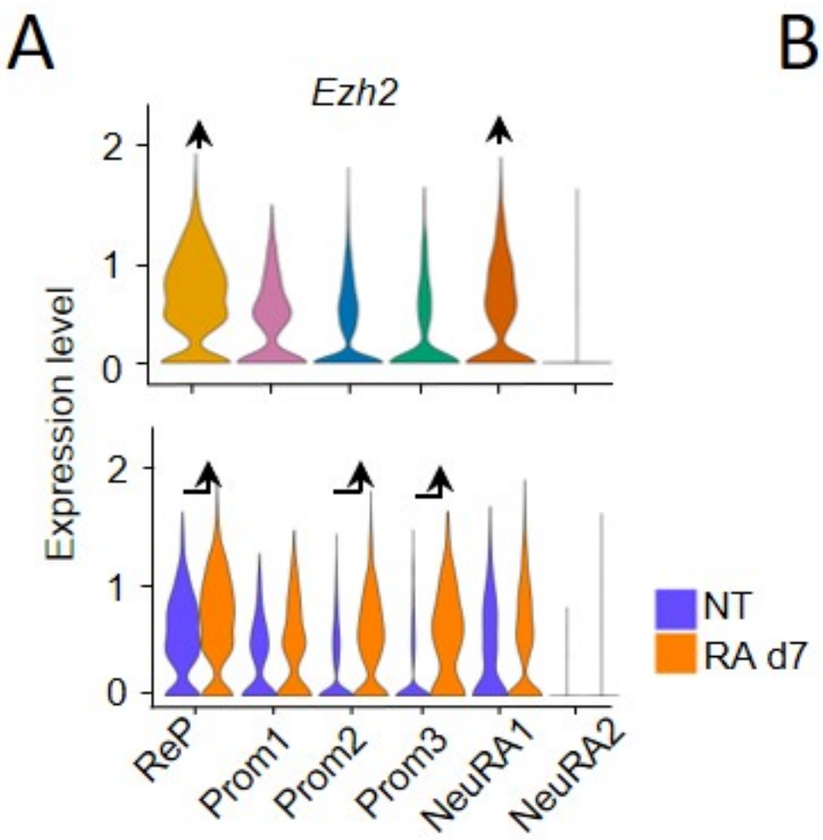
A
Ezh2
Expression level
NT
RA d7
ReP
Prom1
Prom2
Prom3
NeuRA1
NeuRA2

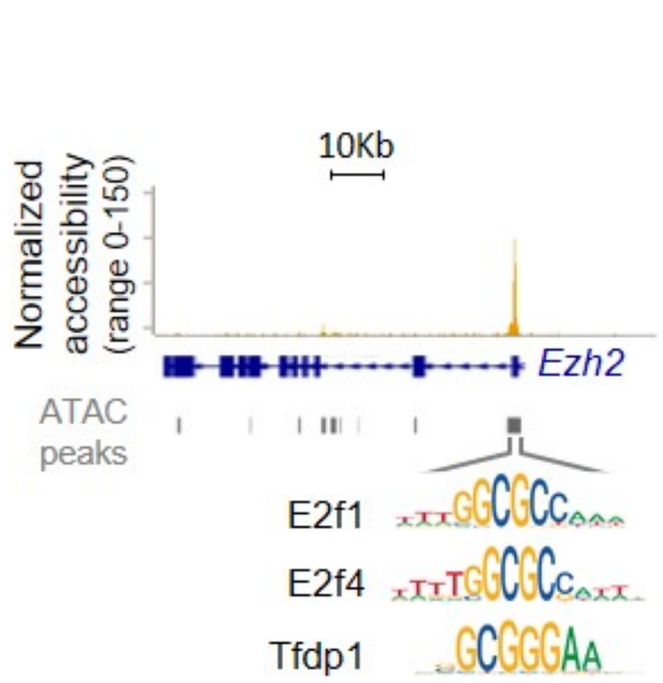
B
10Kb
Normalized accessibility (range 0-150)
Ezh2
ATAC peaks
E2f1
E2f4
Tfdp1

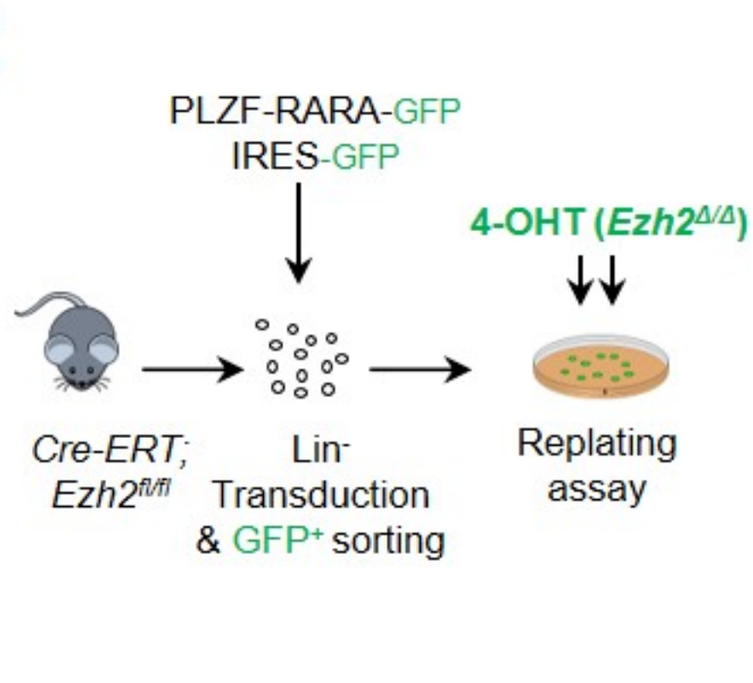
C
PLZF-RARA-GFP
IRES-GFP
4-OHT (Ezh2Δ/Δ)
Cre-ERT; Ezh2fl/fl
Lin- Transduction & GFP+ sorting
Replating assay

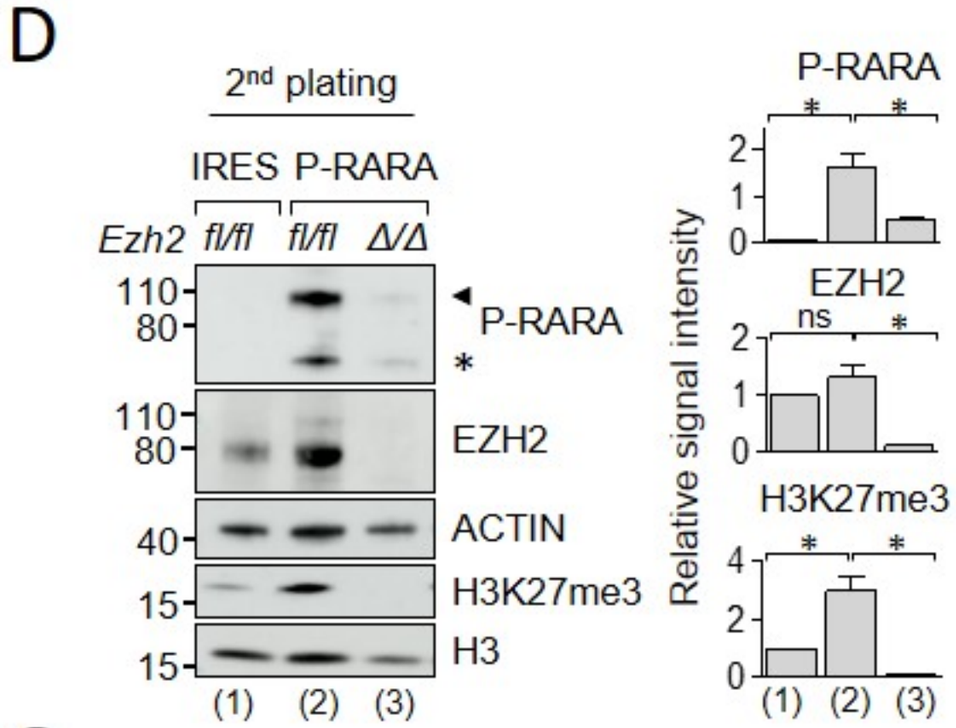
D
2nd plating
IRES P-RARA
Ezh2 fl/fl fl/fl Δ/Δ
P-RARA
EZH2
ACTIN
H3K27me3
H3
Relative signal intensity
(1) (2) (3)

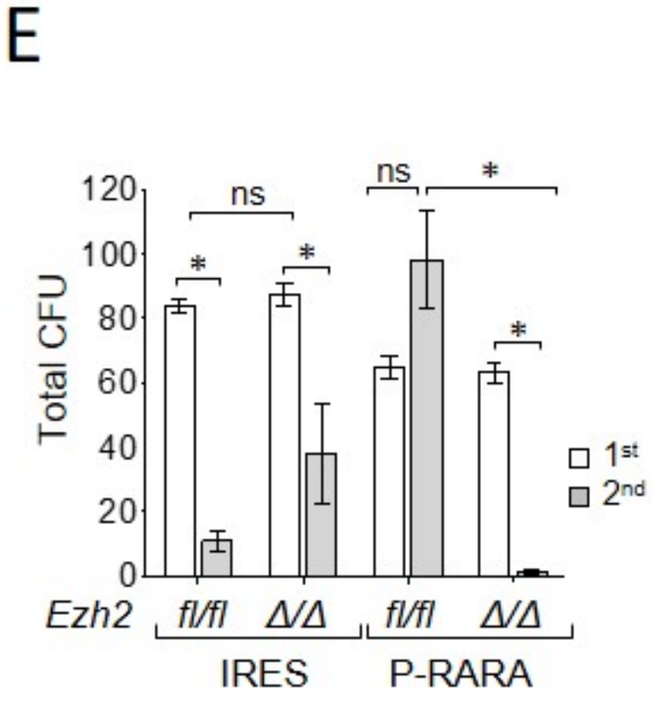
E
Total CFU
1st
2nd
Ezh2 fl/fl Δ/Δ fl/fl Δ/Δ
IRES P-RARA

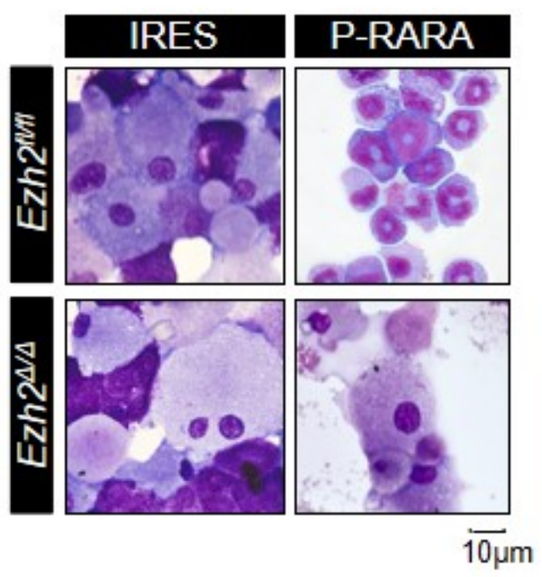
F
IRES
P-RARA
Ezh2fl/fl
Ezh2Δ/Δ
10μm

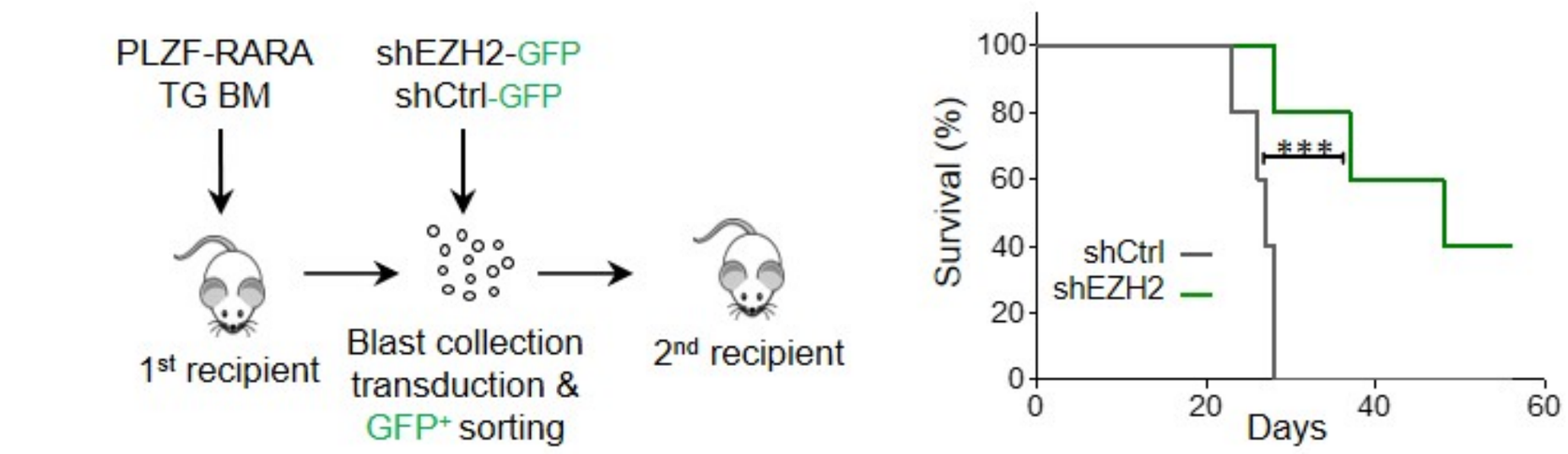
G
PLZF-RARA TG BM
shEZH2-GFP
shCtrl-GFP
1st recipient
Blast collection transduction & GFP+ sorting
2nd recipient

Survival (%)
shCtrl
shEZH2
***
Days

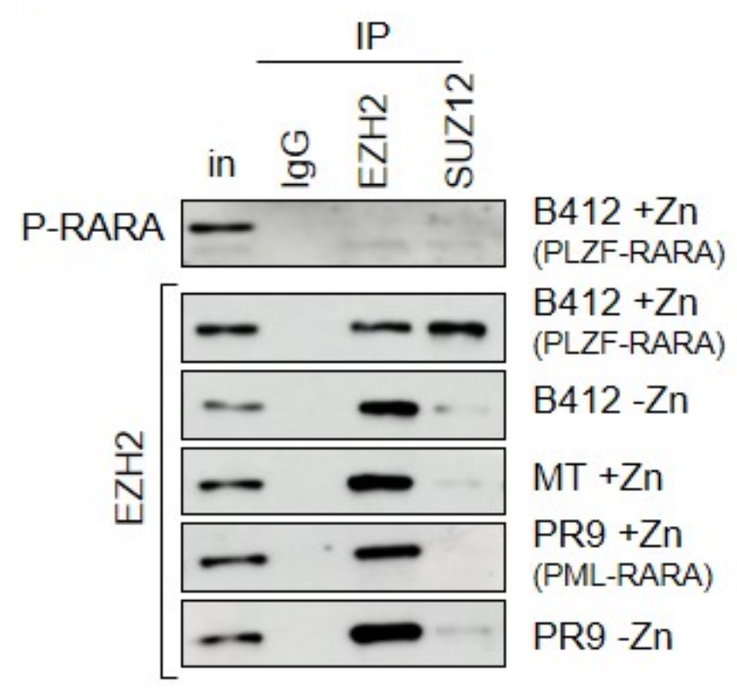
H
IP
in
IgG
EZH2
SUZ12
P-RARA
EZH2
B412 +Zn (PLZF-RARA)
B412 +Zn (PLZF-RARA)
B412 -Zn
MT +Zn
PR9 +Zn (PML-RARA)
PR9 -Zn

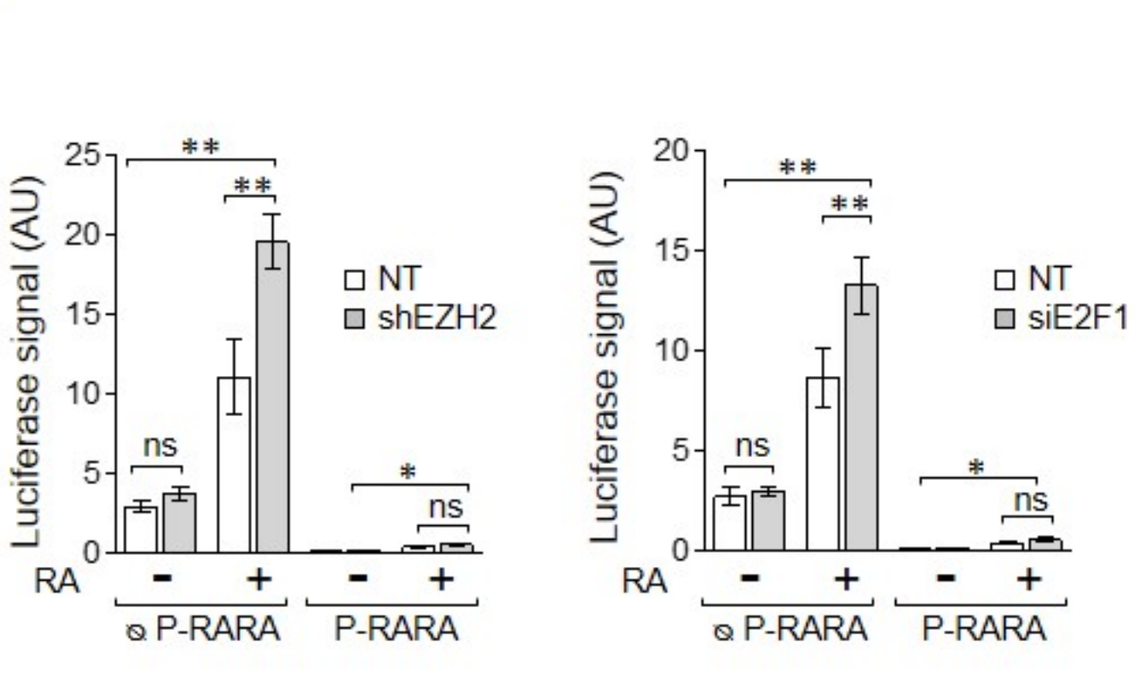
I
Luciferase signal (AU)
NT
shEZH2
siE2F1
RA
⊘ P-RARA
P-RARA

Figure 4

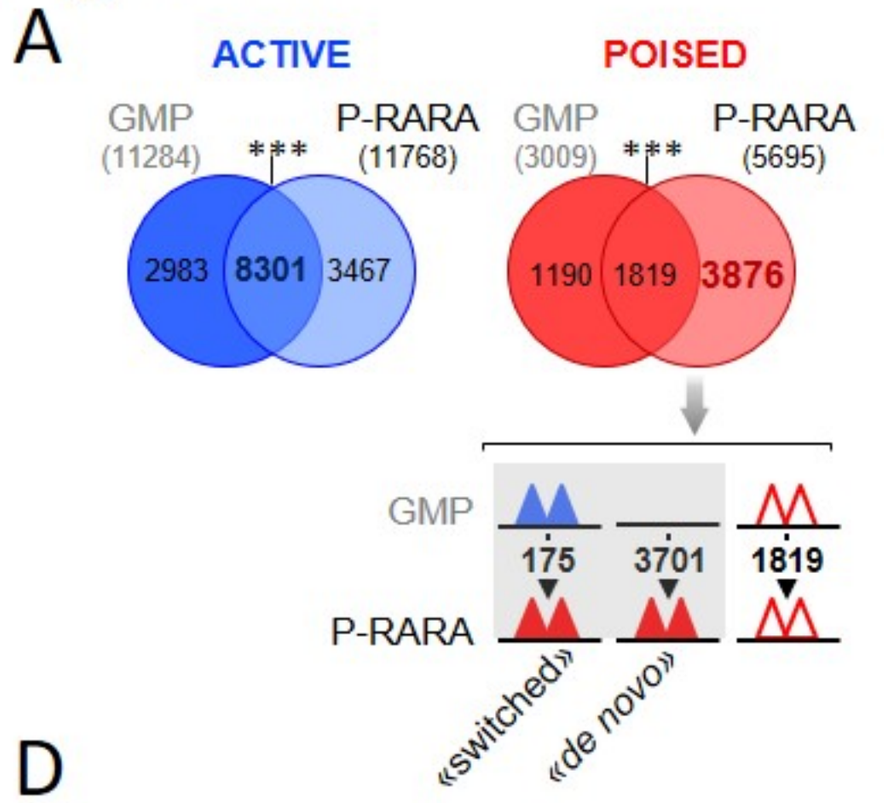
A
ACTIVE
POISED
GMP
(11284)
***
P-RARA
(11768)
2983
8301
3467
GMP
(3009)
***
P-RARA
(5695)
1190
1819
3876
GMP
P-RARA
175
3701
1819
«switched»
«de novo»

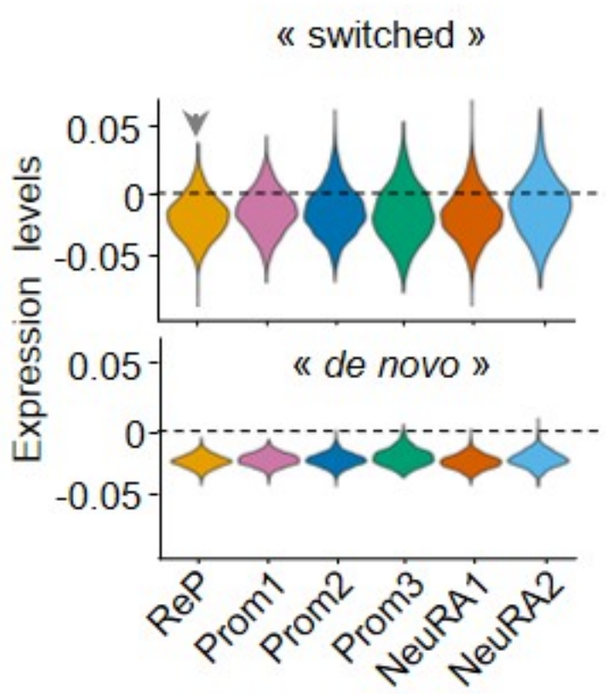
B
« switched »
« de novo »
Expression levels
0.05
0
-0.05
ReP
Prom1
Prom2
Prom3
NeuRA1
NeuRA2

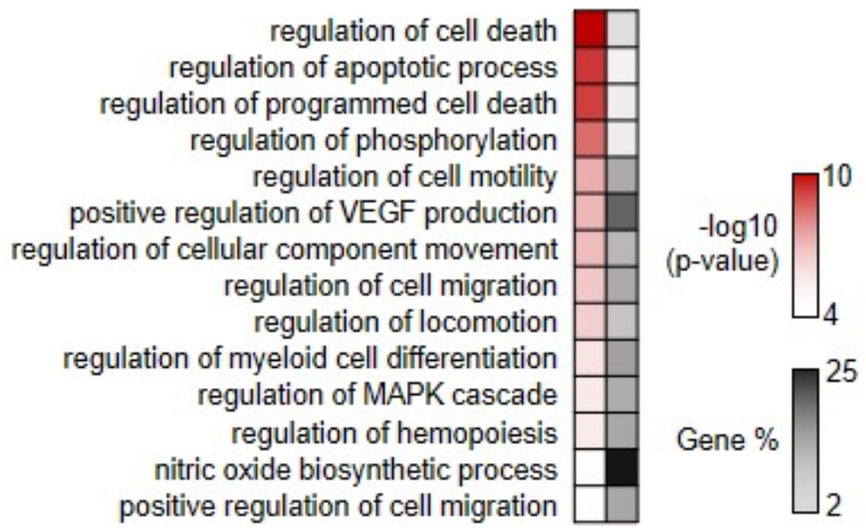
C
GO BP
(Enhancer switch)
regulation of cell death
regulation of apoptotic process
regulation of programmed cell death
regulation of phosphorylation
regulation of cell motility
positive regulation of VEGF production
regulation of cellular component movement
regulation of cell migration
regulation of locomotion
regulation of myeloid cell differentiation
regulation of MAPK cascade
regulation of hemopoiesis
nitric oxide biosynthetic process
positive regulation of cell migration
-log10
(p-value)
10
4
Gene %
25
2

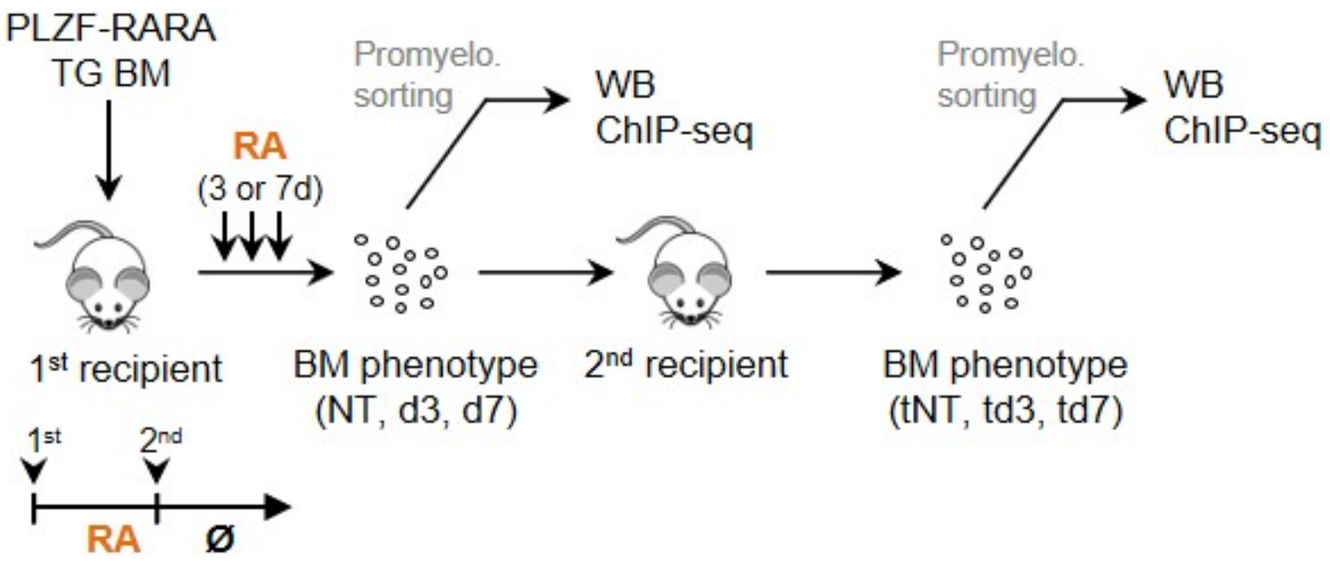
D
PLZF-RARA
TG BM
RA
(3 or 7d)
Promyelo.
sorting
WB
ChIP-seq
1st recipient
BM phenotype
(NT, d3, d7)
2nd recipient
BM phenotype
(tNT, td3, td7)
1st
2nd
RA
Ø

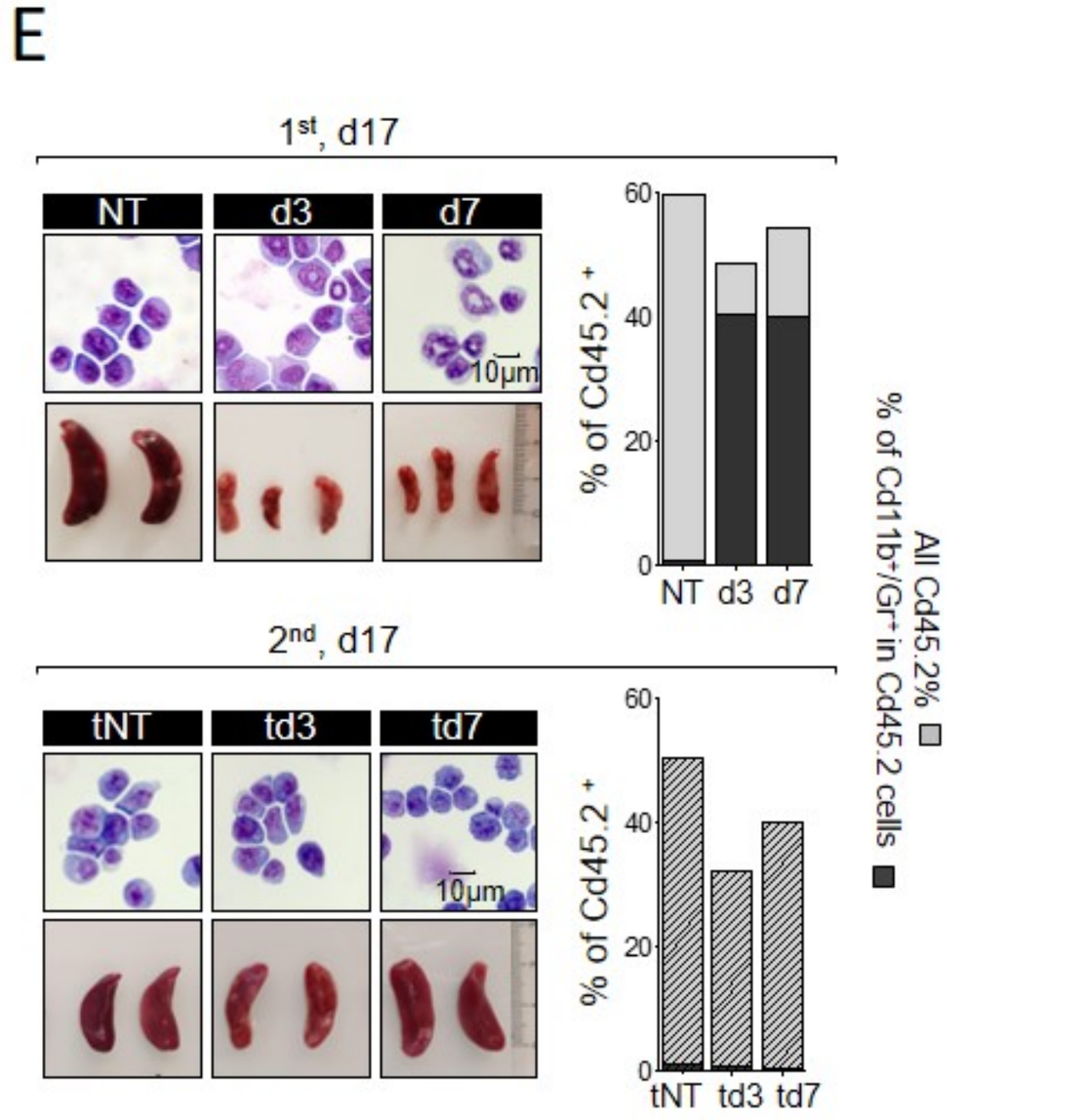
E
1st, d17
NT
d3
d7
10µm
% of Cd45.2 +
NT d3 d7
2nd, d17
tNT
td3
td7
tNT td3 td7
All Cd45.2% □
% of Cd11b+/Gr+ in Cd45.2 cells ■

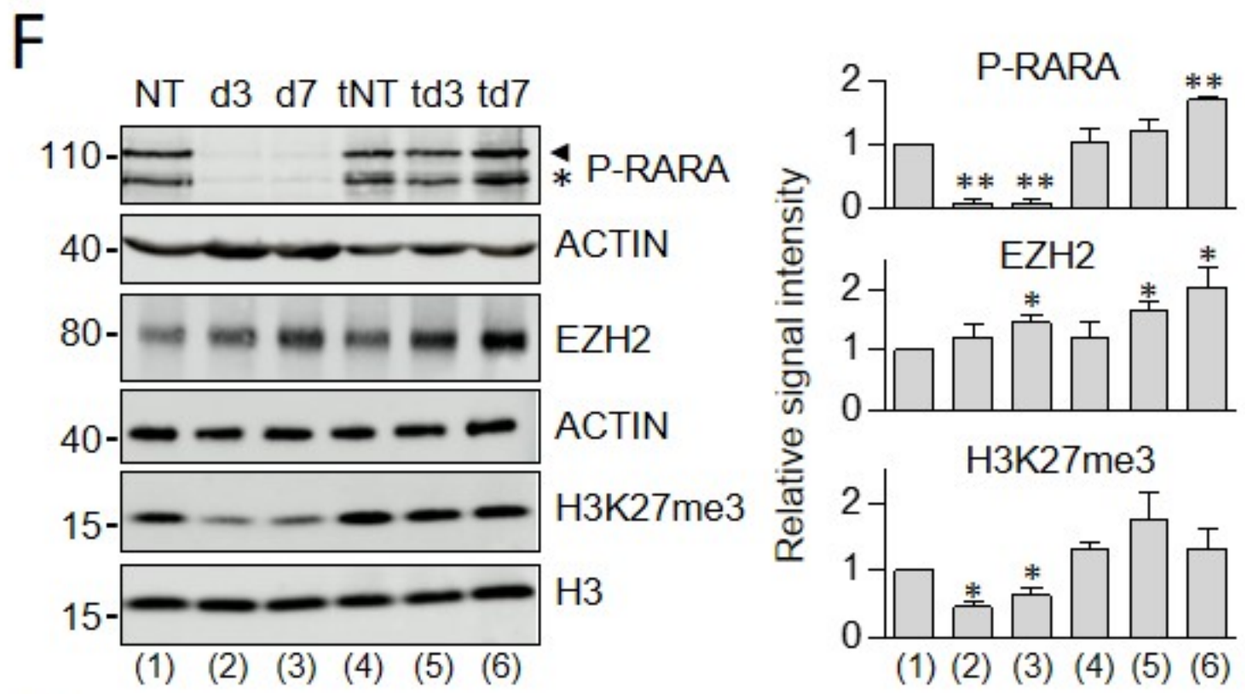
F
NT d3 d7 tNT td3 td7
110
P-RARA
40
ACTIN
80
EZH2
15
H3K27me3
15
H3
(1) (2) (3) (4) (5) (6)
Relative signal intensity
P-RARA
EZH2
H3K27me3

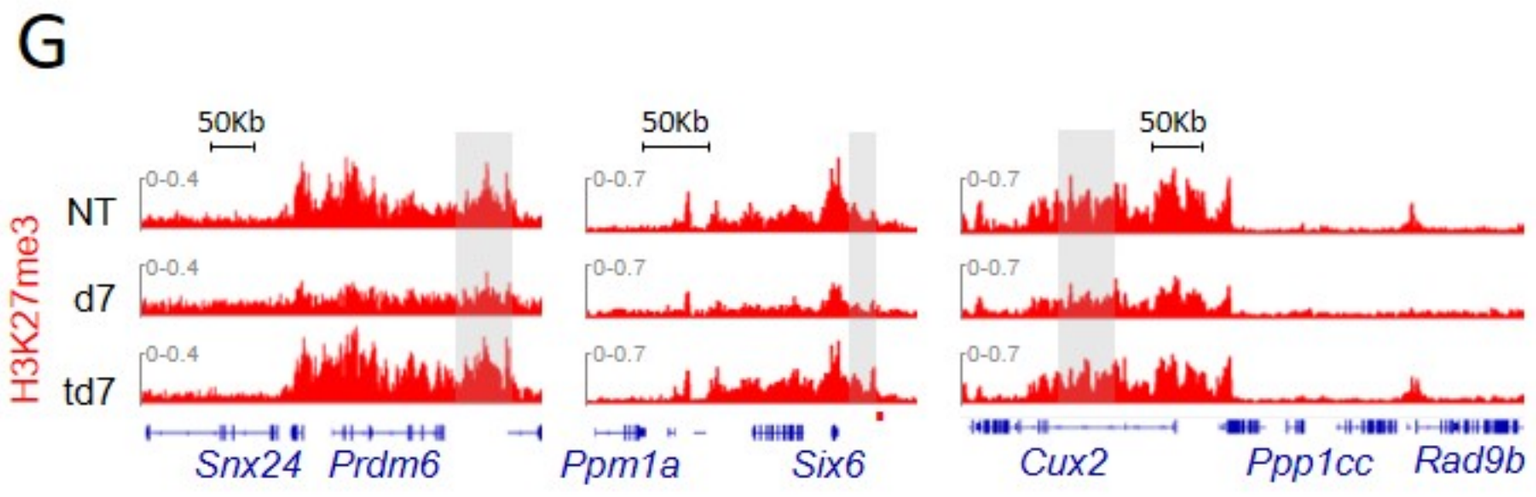
G
50Kb
H3K27me3
NT
d7
td7
0-0.4
0-0.7
Snx24
Prdm6
Ppm1a
Six6
Cux2
Ppp1cc
Rad9b

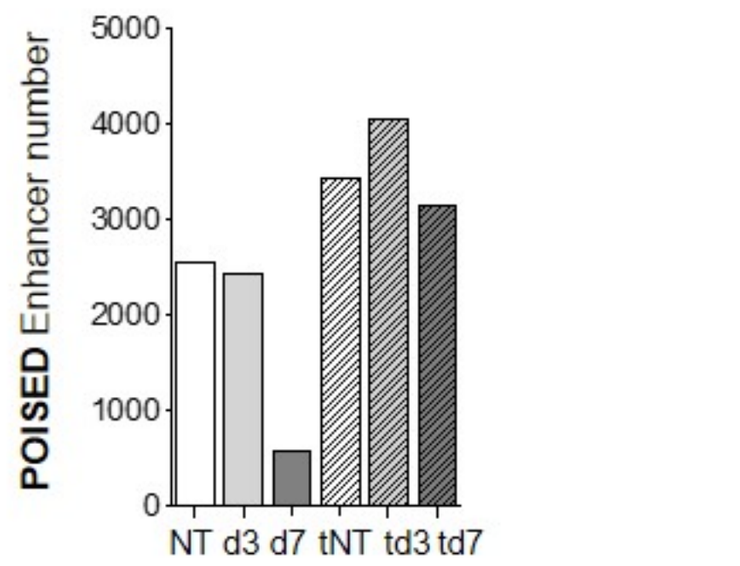
H
POISED Enhancer number
5000
4000
3000
2000
1000
0
NT d3 d7 tNT td3 td7

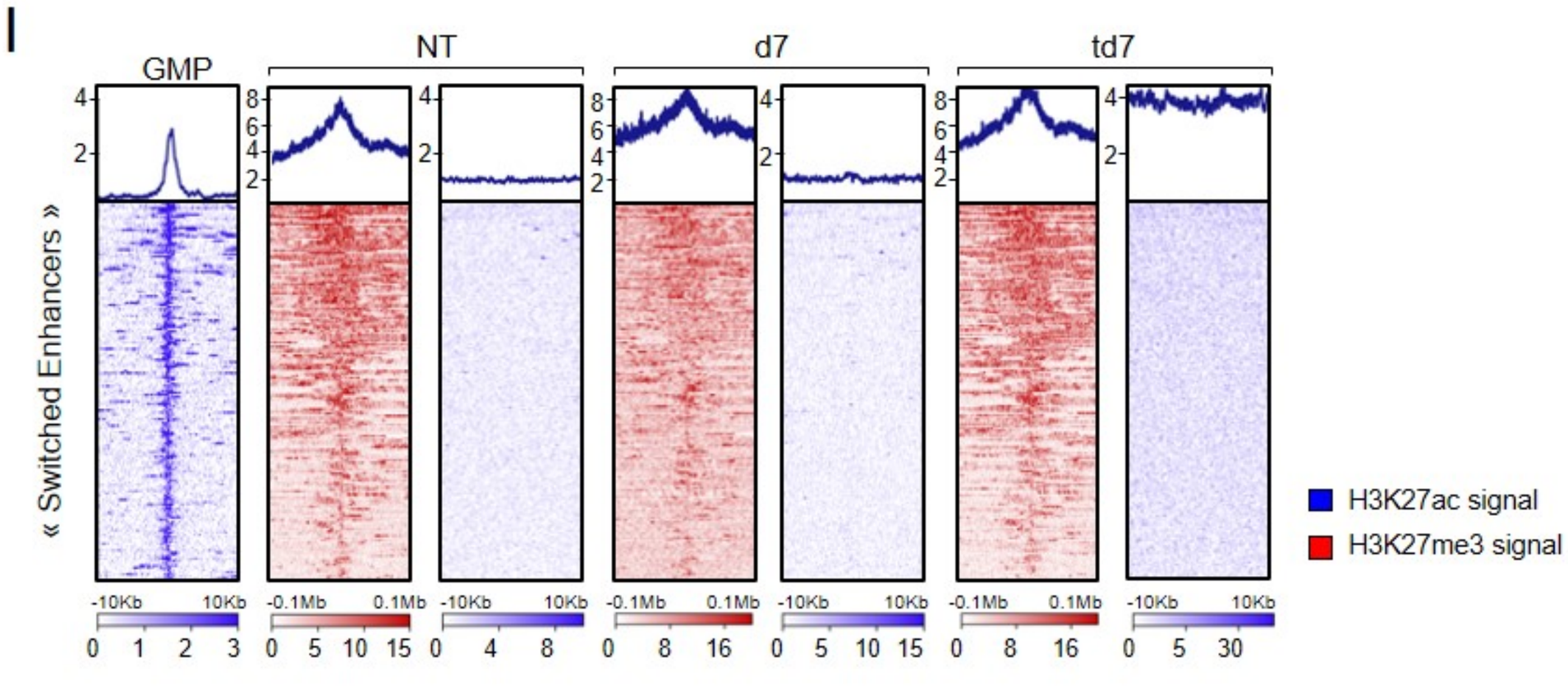
I
« Switched Enhancers »
GMP
NT
d7
td7
-10Kb
10Kb
-0.1Mb
0.1Mb
H3K27ac signal
H3K27me3 signal

Figure 5

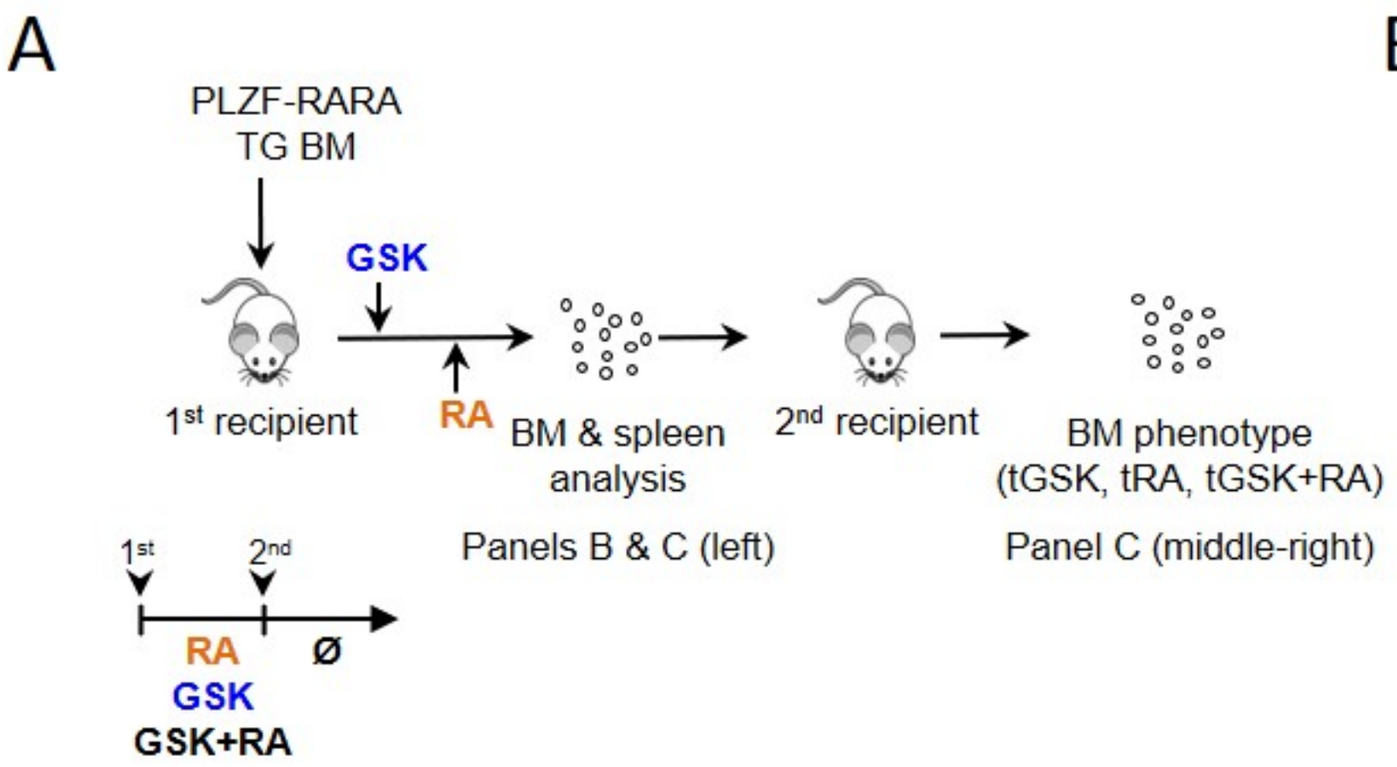
A
PLZF-RARA
TG BM
GSK
RA
1st recipient
BM & spleen
analysis
2nd recipient
BM phenotype
(tGSK, tRA, tGSK+RA)
Panels B & C (left)
Panel C (middle-right)
1st
2nd
RA
Ø
GSK
GSK+RA

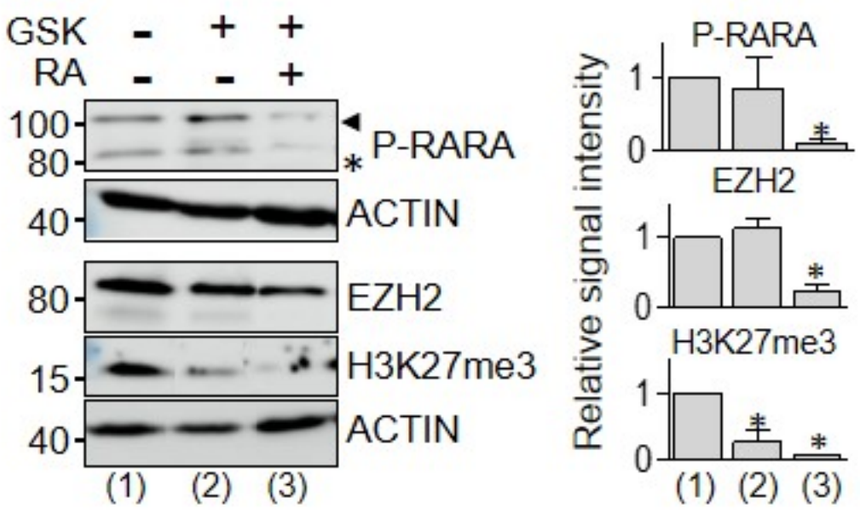
B
GSK - + +
RA - - +
100
80
40
80
15
40
P-RARA
ACTIN
EZH2
H3K27me3
ACTIN
(1) (2) (3)
Relative signal intensity
P-RARA
EZH2
H3K27me3
1
0
(1) (2) (3)

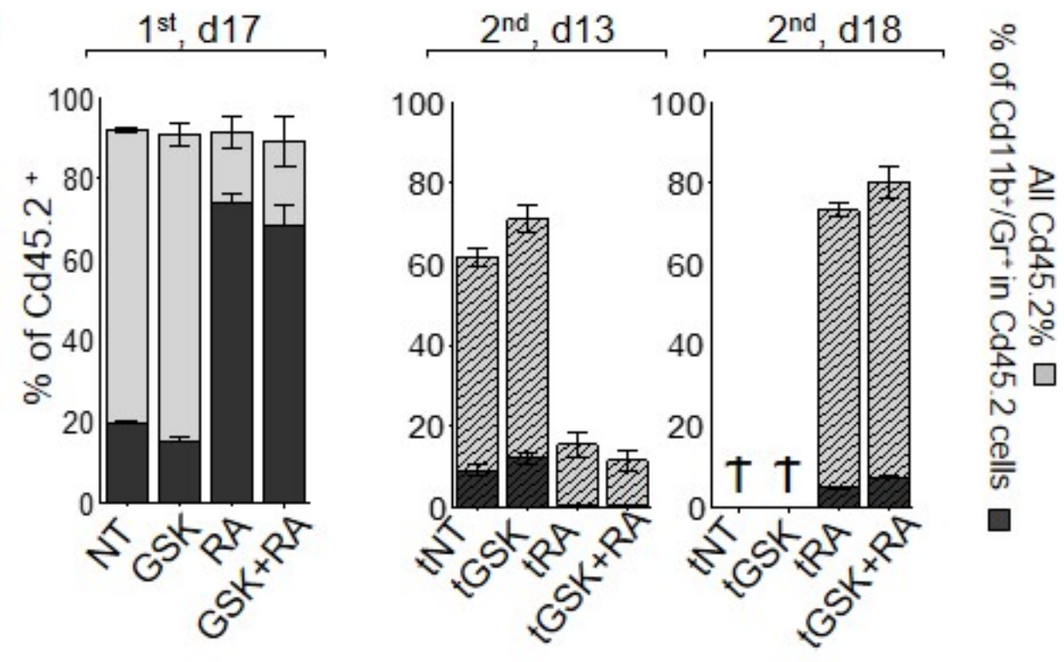
C
1st, d17
2nd, d13
2nd, d18
% of Cd45.2 +
100
80
60
40
20
0
NT
GSK
RA
GSK+RA
tNT
tGSK
tRA
tGSK+RA
† †
All Cd45.2% □
% of Cd11b+/Gr+ in Cd45.2 cells ■

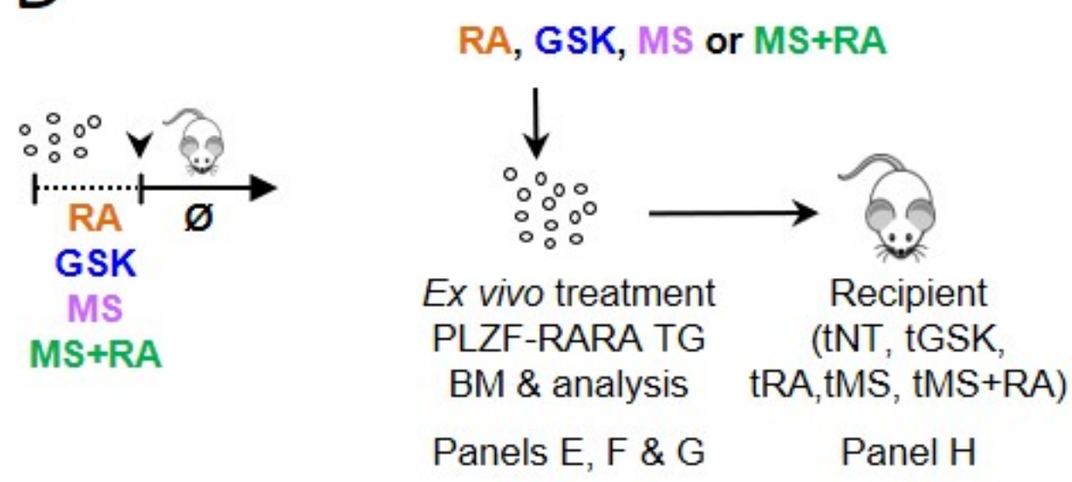
D
RA
GSK
MS
MS+RA
Ø
RA, GSK, MS or MS+RA
Ex vivo treatment
PLZF-RARA TG
BM & analysis
Recipient
(tNT, tGSK,
tRA,tMS, tMS+RA)
Panels E, F & G
Panel H

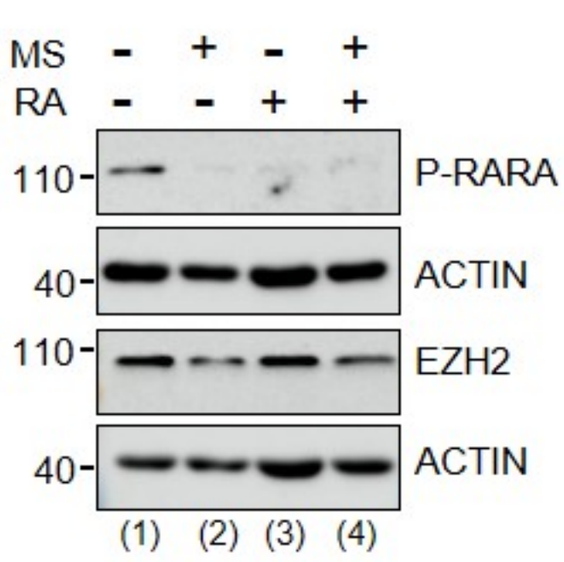
E
MS - + - +
RA - - + +
110
40
110
40
P-RARA
ACTIN
EZH2
ACTIN
(1) (2) (3) (4)

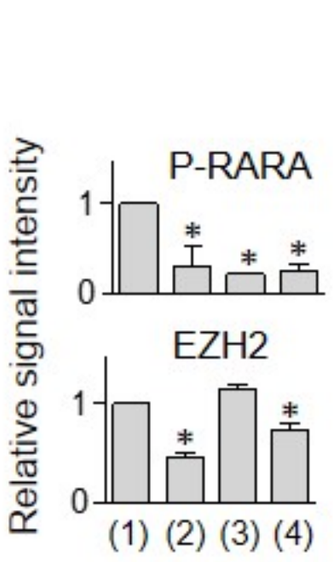
Relative signal intensity
P-RARA
EZH2
1
0
(1) (2) (3) (4)

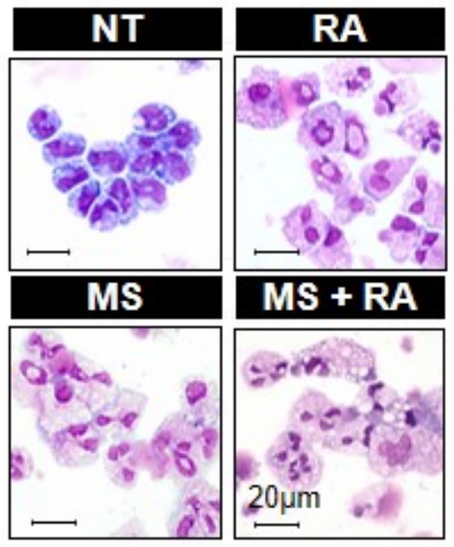
F
NT
RA
MS
MS + RA
20µm

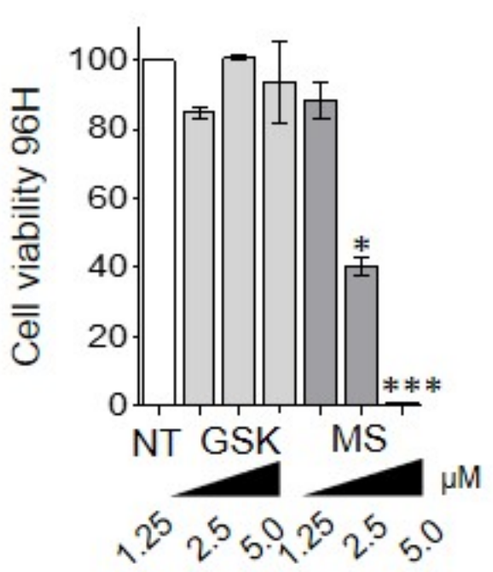
G
Cell viability 96H
100
80
60
40
20
0
***
NT GSK MS
µM
1.25 2.5 5.0 1.25 2.5 5.0

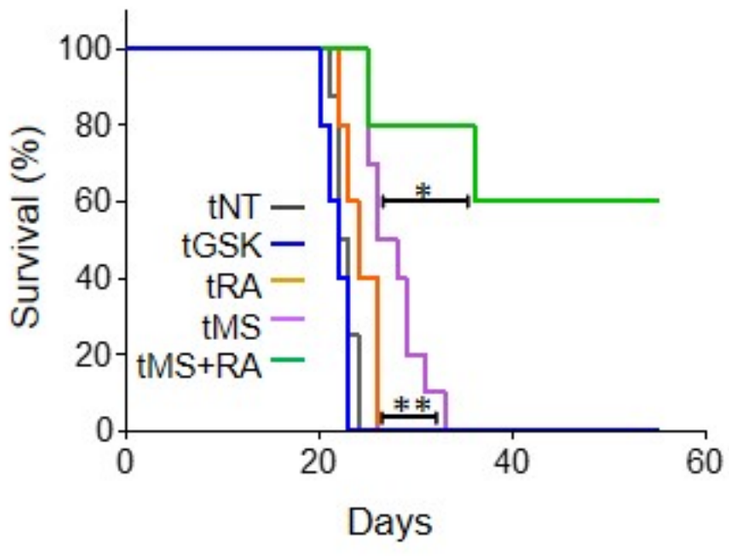
H
Survival (%)
100
80
60
40
20
0
tNT
tGSK
tRA
tMS
tMS+RA
*
**
0
20
40
60
Days

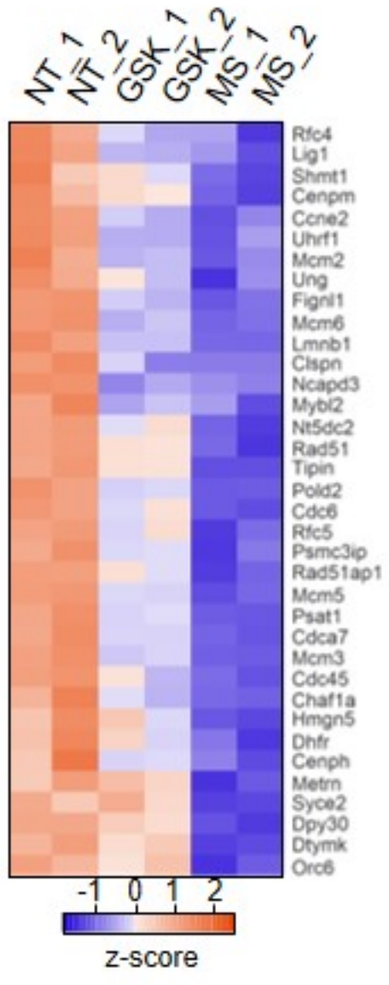
I
NT_1
NT_2
GSK_1
GSK_2
MS_1
MS_2
Rfc4
Lig1
Shmt1
Cenpm
Ccne2
Uhrf1
Mcm2
Ung
Fignl1
Mcm6
Lmnb1
Clspn
Ncapd3
Mybl2
Nt5dc2
Rad51
Tipin
Pold2
Cdc6
Rfc5
Psmc3ip
Rad51ap1
Mcm5
Psat1
Cdca7
Mcm3
Cdc45
Chaf1a
Hmgn5
Dhfr
Cenph
Metrn
Syce2
Dpy30
Dtymk
Orc6
-1 0 1 2
z-score

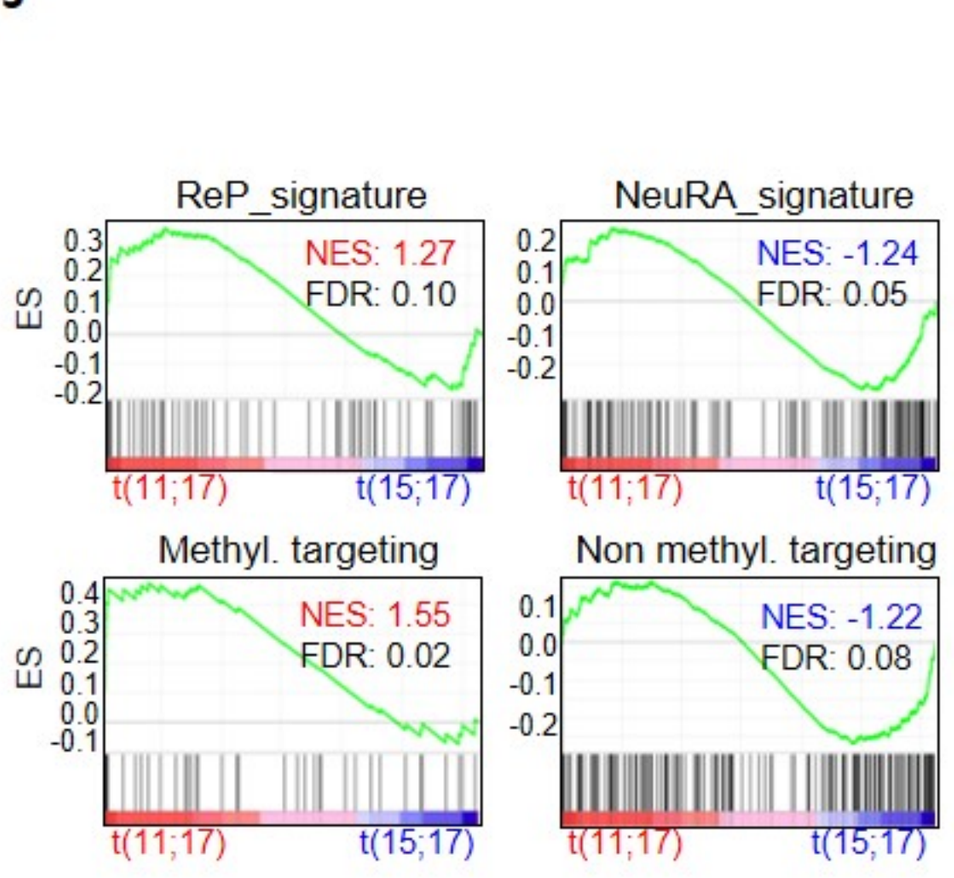
J
ReP_signature
NES: 1.27
FDR: 0.10
NeuRA_signature
NES: -1.24
FDR: 0.05
Methyl. targeting
NES: 1.55
FDR: 0.02
Non methyl. targeting
NES: -1.22
FDR: 0.08
ES
t(11;17)
t(15;17)